University of Stuttgart
Institute for Materials Science

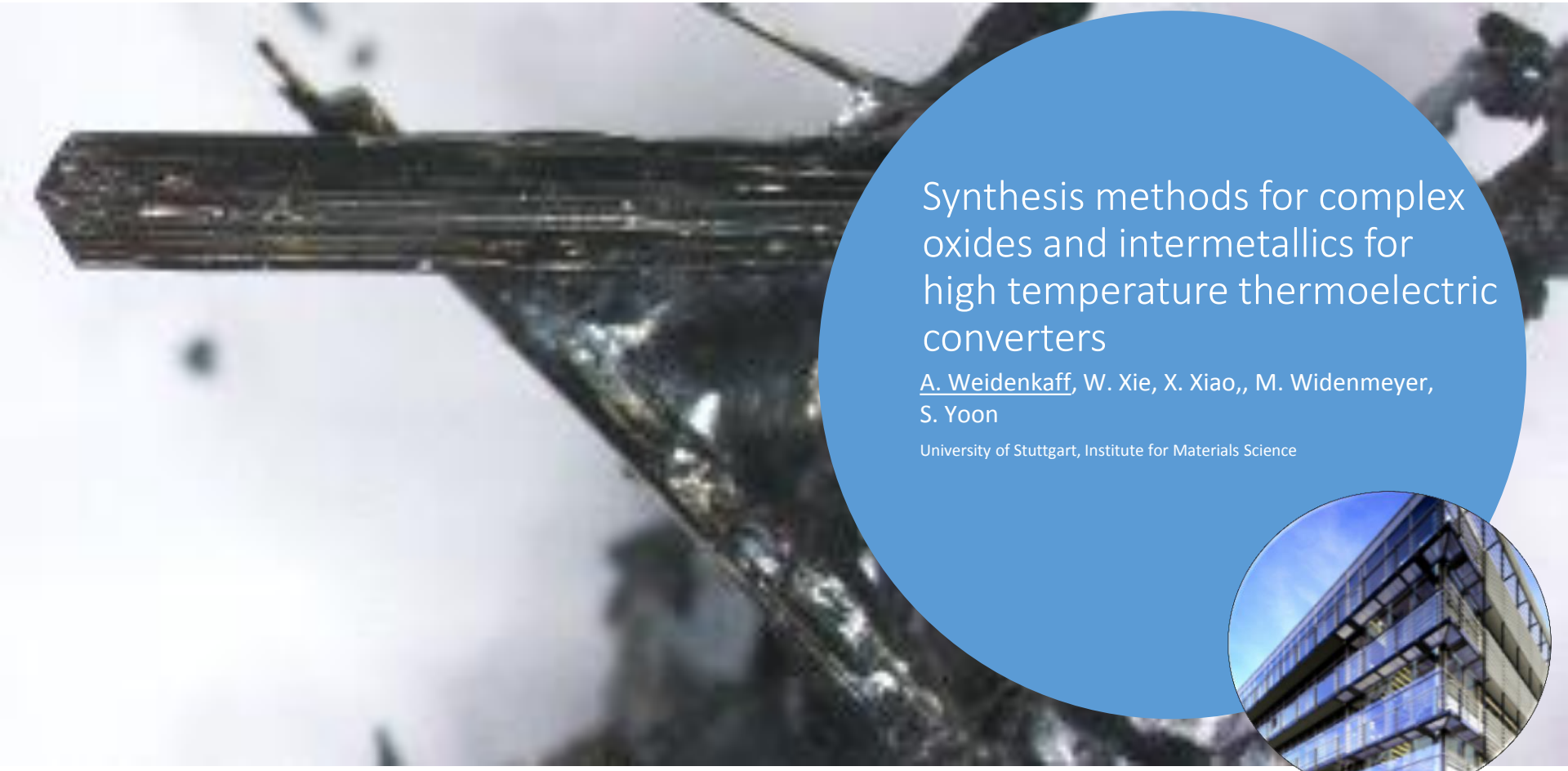

Synthesis methods for complex oxides and intermetallics for high temperature thermoelectric converters

A. Weidenkaff, W. Xie, X. Xiao,, M. Widenmeyer, S. Yoon

University of Stuttgart, Institute for Materials Science

EPSRC Thermoelectric Network

Thermoelectric Network Meeting Manchester 14-15 February 2017

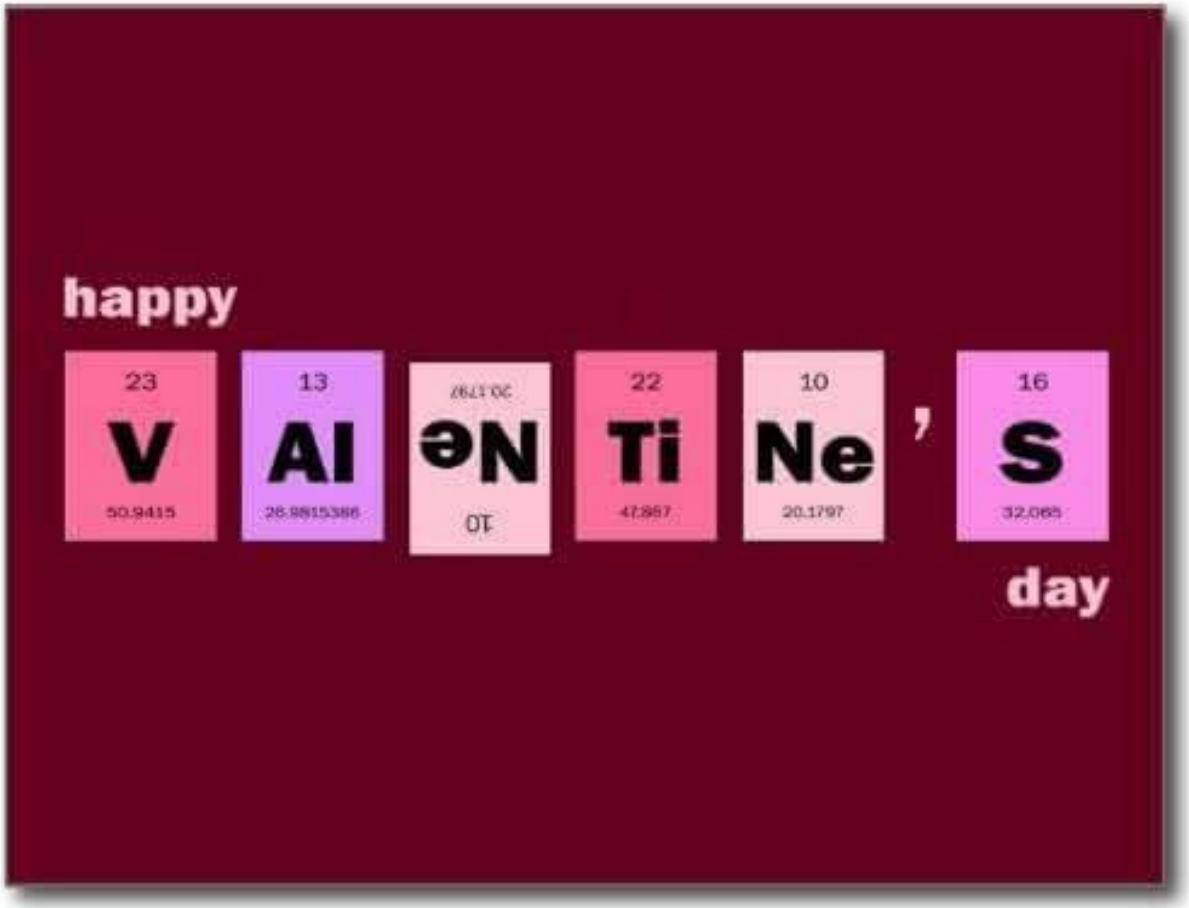
happy
23
V
50.9415
13
Al
26.9815386
10
Ne
20.1797
22
Ti
47.867
10
Ne
20.1797
'
16
S
32.065
day

Motivation

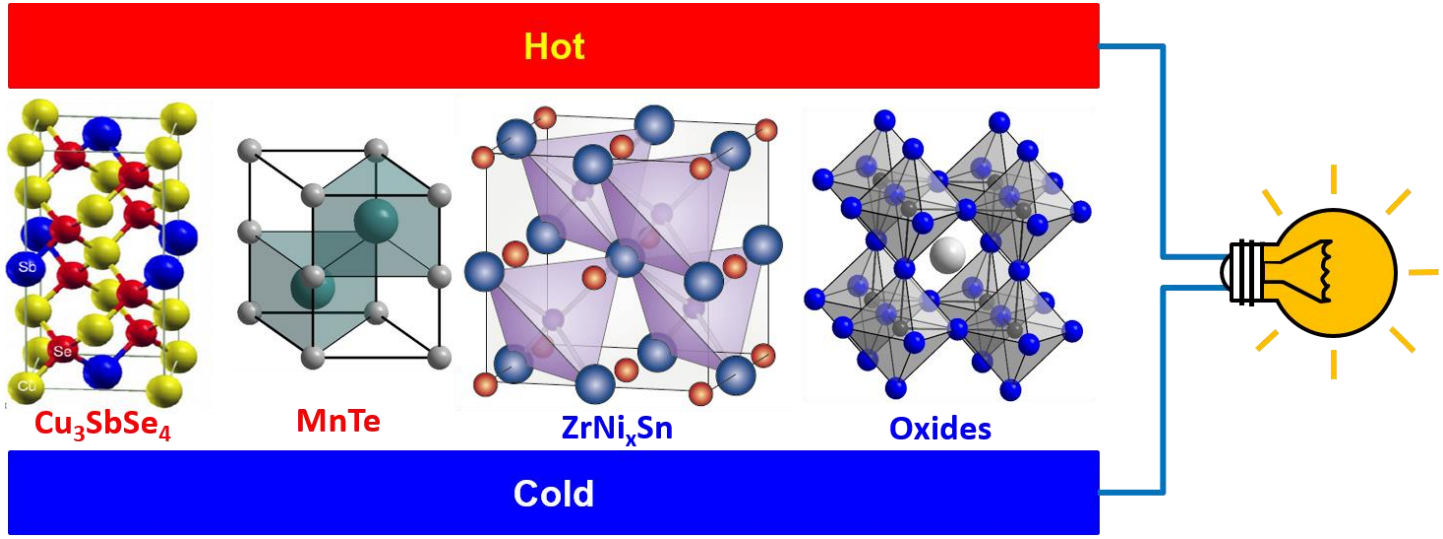

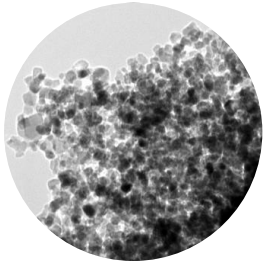

- Structure property relation
- High Temperature Ceramic Converters
- Soft-chemistry synthesis
- Perovskite-type Titanates
- Half-Heusler Materials

Tailoring of TE materials

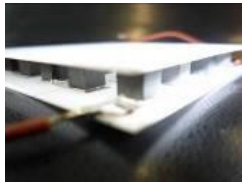

>1W/cm²

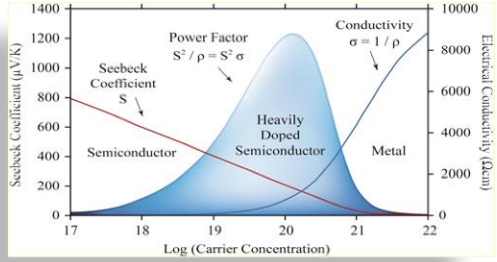

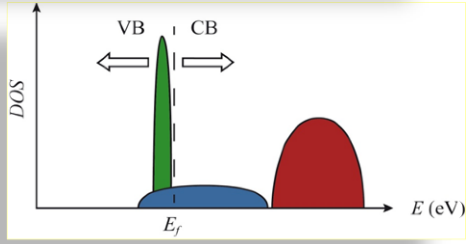

test

Design rules

applications

- High thermal heat flow conversion vs. thermal insulation
- transp.prop., regenerativity, ..

characterisation

- DoS, structure, comp.
- Defect structure
- Dynamic behavior

materials choice

- PGEC
- perovskites-type oxides
- heusler compounds

function, form, scalability

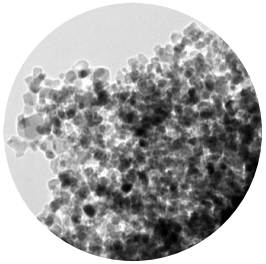

synthesis

- "chimie douce", USC, flame spray, flux, MW, plasma
- Homogenation, densification
- Single Crystals

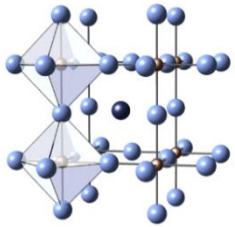

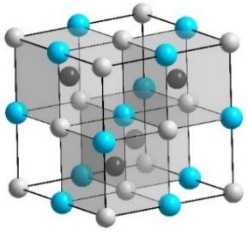

HT Synthesis and Characterisation Equipment

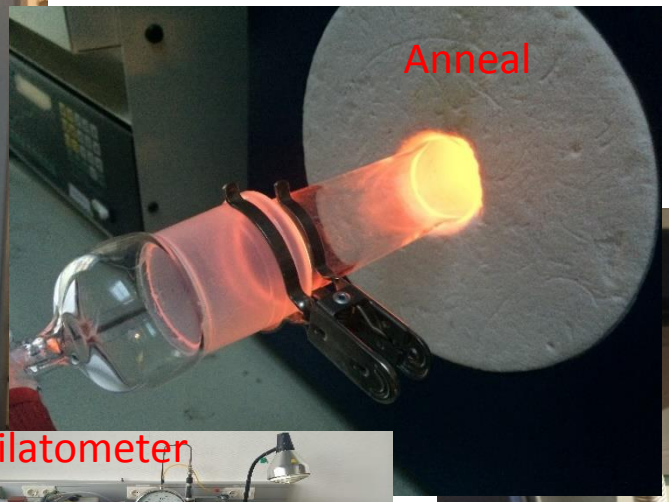

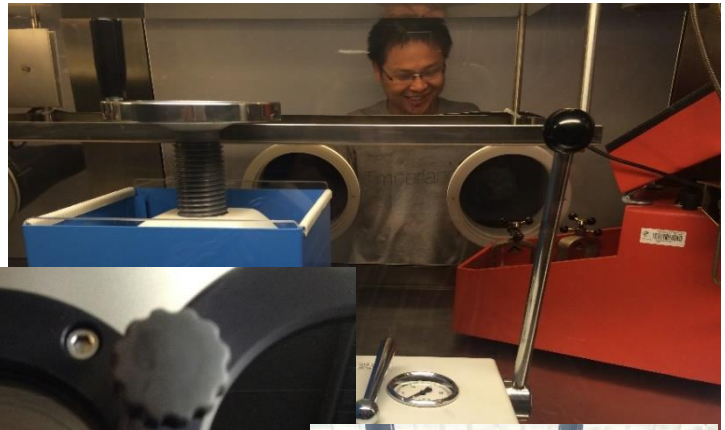

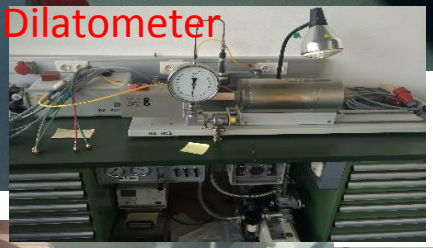

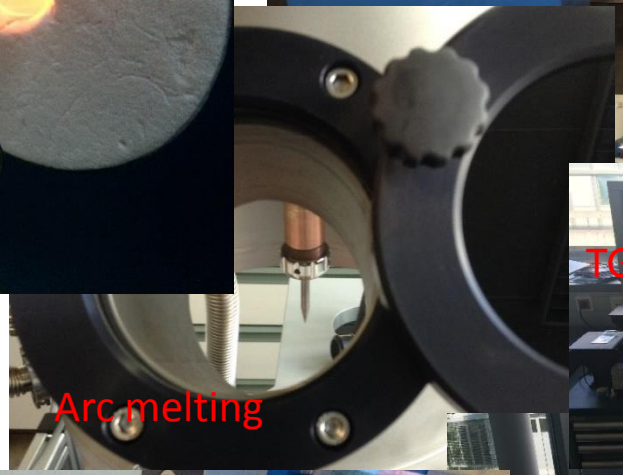

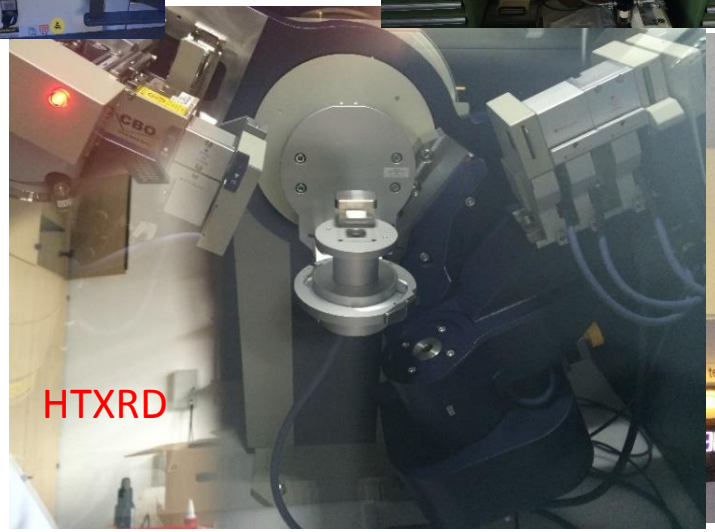

Materials Synthesis Directed by Biological Templates

- Biomineralization of materials with microalgae

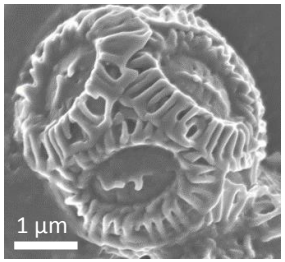

- Mineralization using specifically interacting peptides

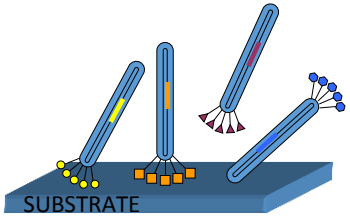

- Nano-structuring with bio-templates

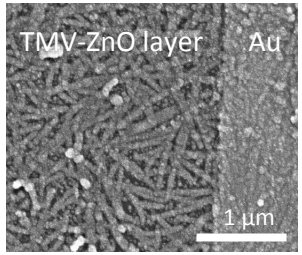

- Biomineral structures as models for new functions

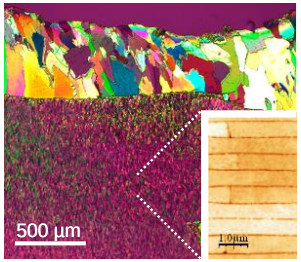

Stability tests (>100h)

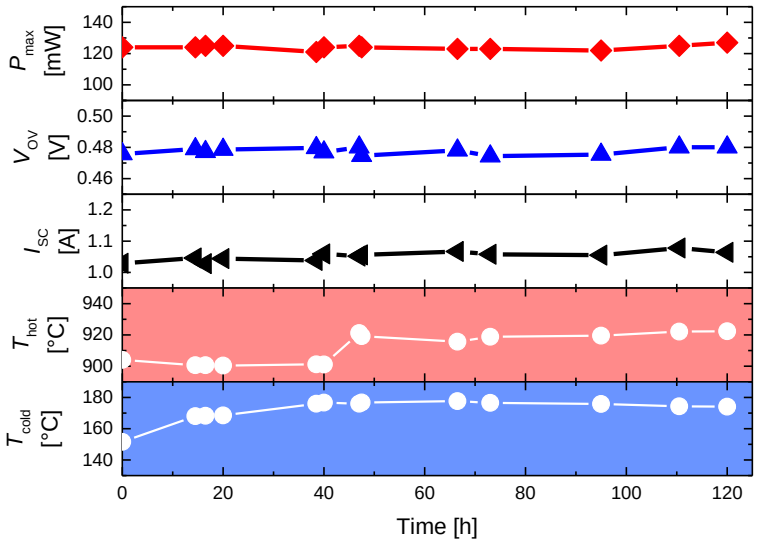

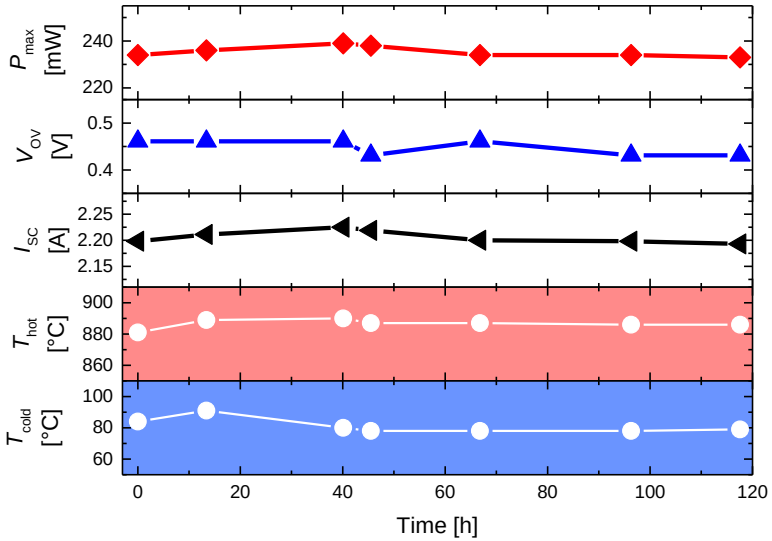

- High power density:
  1.4 W/cm^3
- No degradation during 110 h of high temperature thermoelectric conversion

Saucke, G., Populoh, S., Thiel,P., Xie, W., Funahashi, R. and Weidenkaff, A., Journal of Applied Physics, 118, (2015) 035106.

Experimental

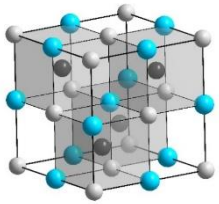

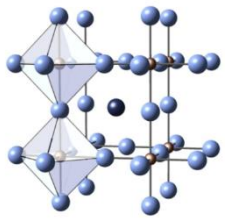

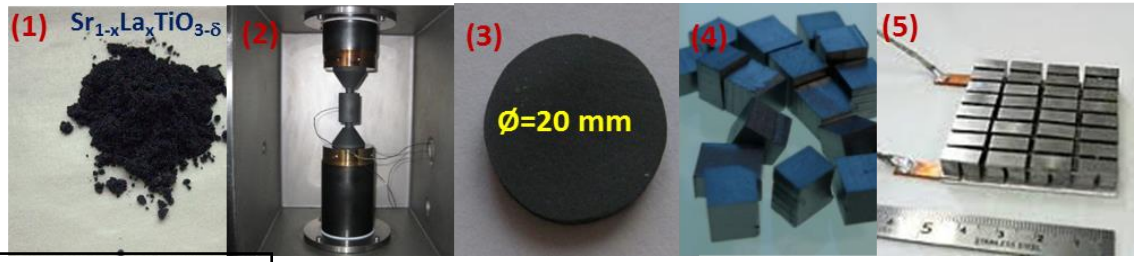

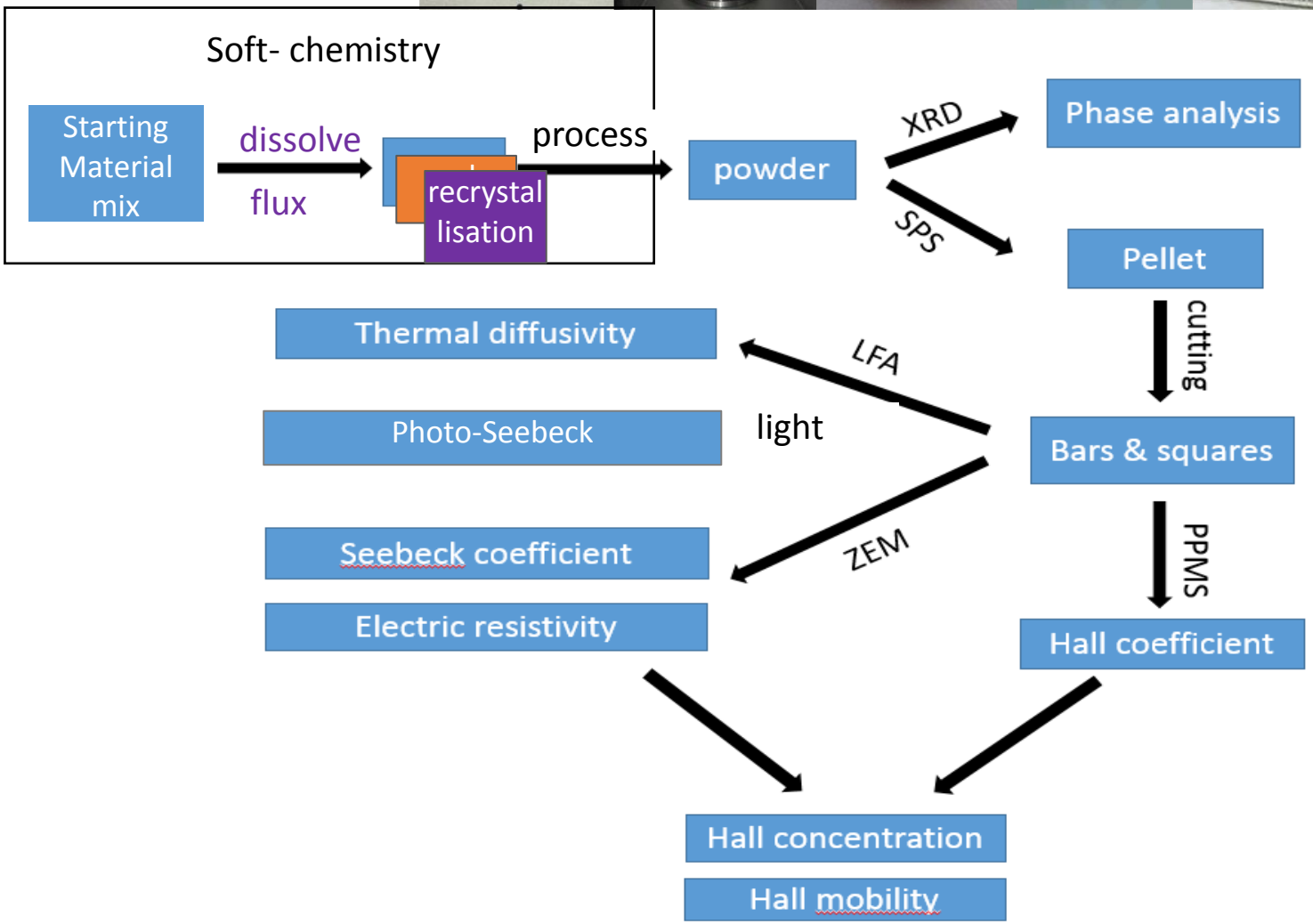

W. Xie, T. Zou

Titanates: $EuTiO_3$ ceramics

- Perovskite structure ABO_3 ($Pm\bar{3}m$ symmetry)
- Structural distortion below RT [1]

Eu^{2+}

4*f* localized electrons
AFM ordering at 5.3 K
Strong spin-lattice coupling

Ti^{4+}

Transition metal
3*d* electrons
Strongly correlated electrons

O^{2-}

octahedron

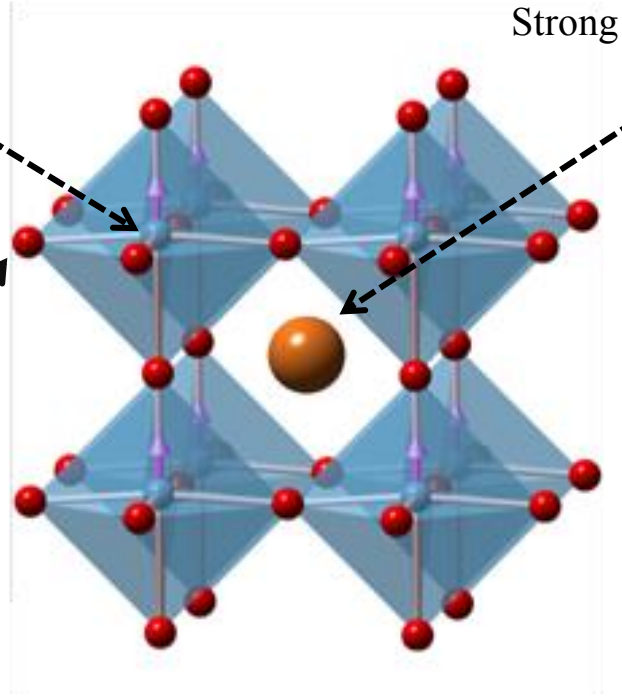

ABX_3

Competing Instabilities in EuTiO3, *PRL* **110**, (2013) 027201.

Antiferrodistortive phase transition in EuTiO3, **Phys. Rev. B 86, 054112 (2012)**

Localized Eu 4*f* electron band

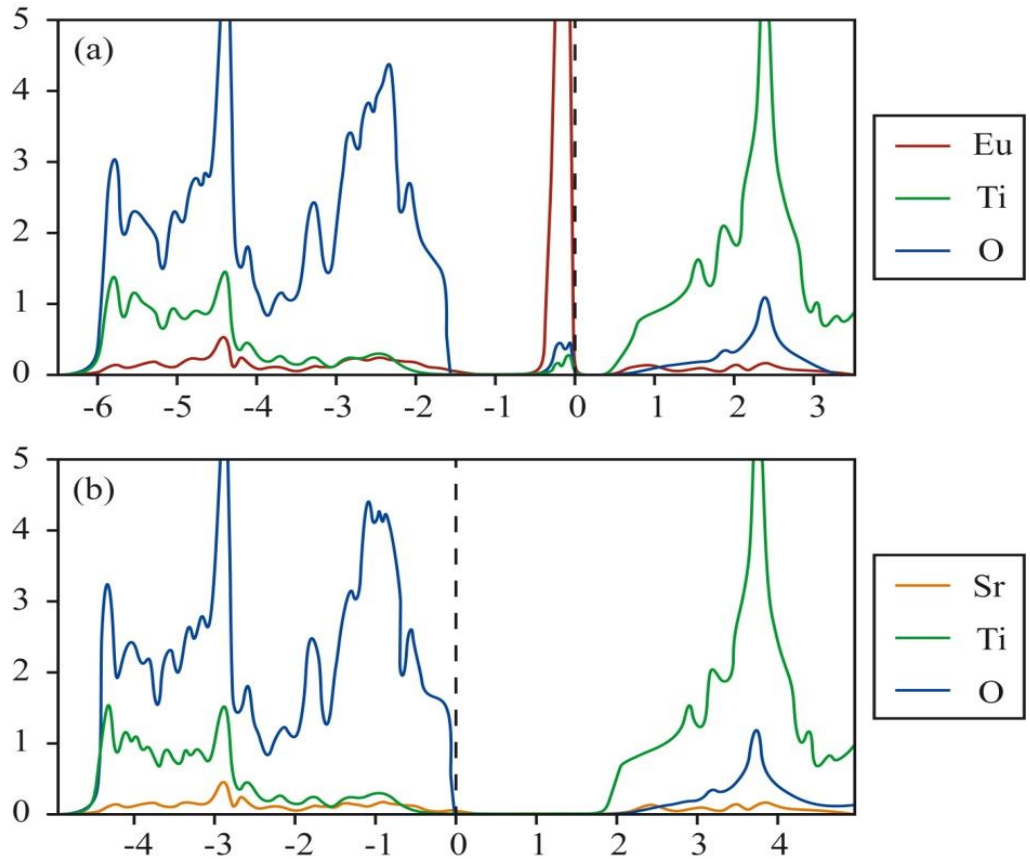

$EuTiO_3$

- Band gap < 1 eV
- Localized Eu 4*f* electron band near the Fermi level → high Seebeck coefficient $S \propto [\partial \ln n(E)/\partial E]_{E=E_F}$.

Vienna *ab-initio* Simulation Package (VASP) code, Heyd-Scuseria-Ernzerhof (HSE) hybrid functional

L. Sagarna, K.Z. Rushchanskii, A. Maegli, S. Yoon, S. Populoh, A. Shkabko, et al., *J. Appl. Phys*. **114** (2013) 033701

Thermoelectric properties of $EuTiO_{3-\delta}$ & $EuTi_{0.98}Nb_{0.02}O_{3-\delta}$

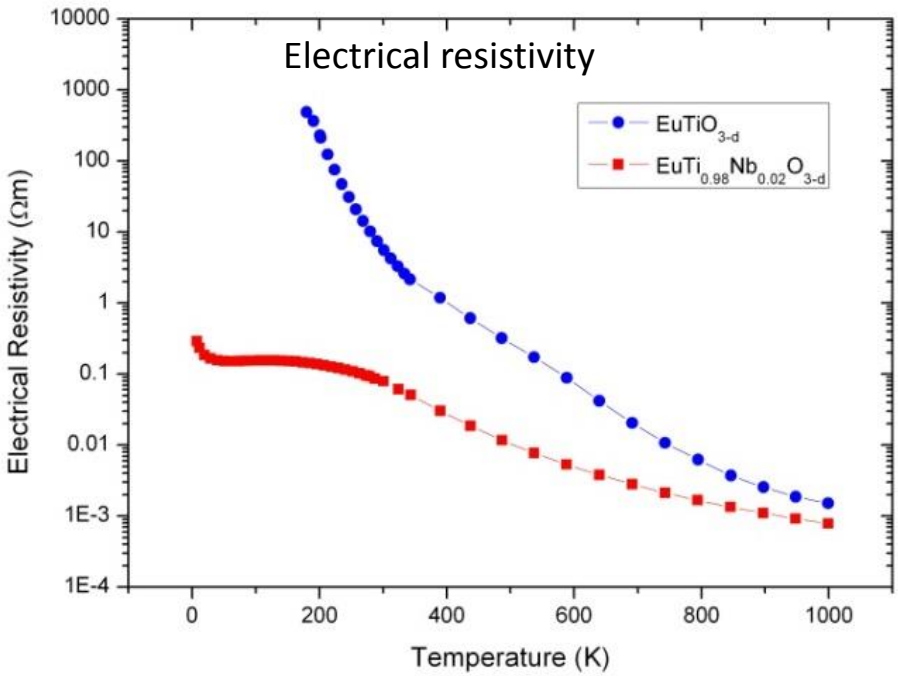

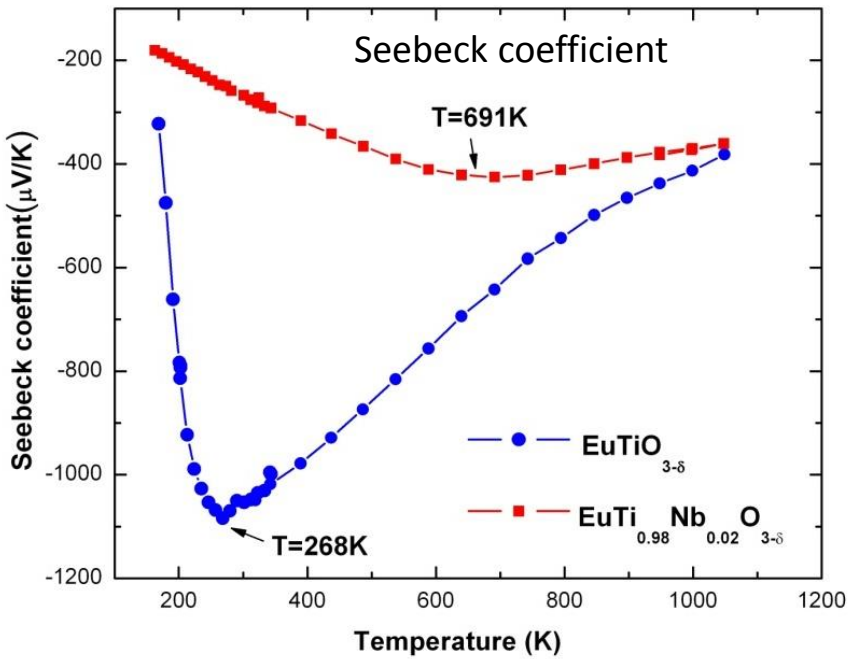

- Decrease of σ by Nb 2% substitution: one order of magnitude at high T
- $EuTiO_3$ is one of the oxides with highest $|S|$ = 1081 μV/K at T = 268 K

-> n-type thermoelectric leg material

L. Sagarna et al, *Appl. Phys. Lett.* **101**, *APL* (2012) 033908

$EuTiO_3$: One of the best perovskite-type TE materials

Figure of Merit:

$$ZT = \frac{S^2\sigma}{\kappa} T$$

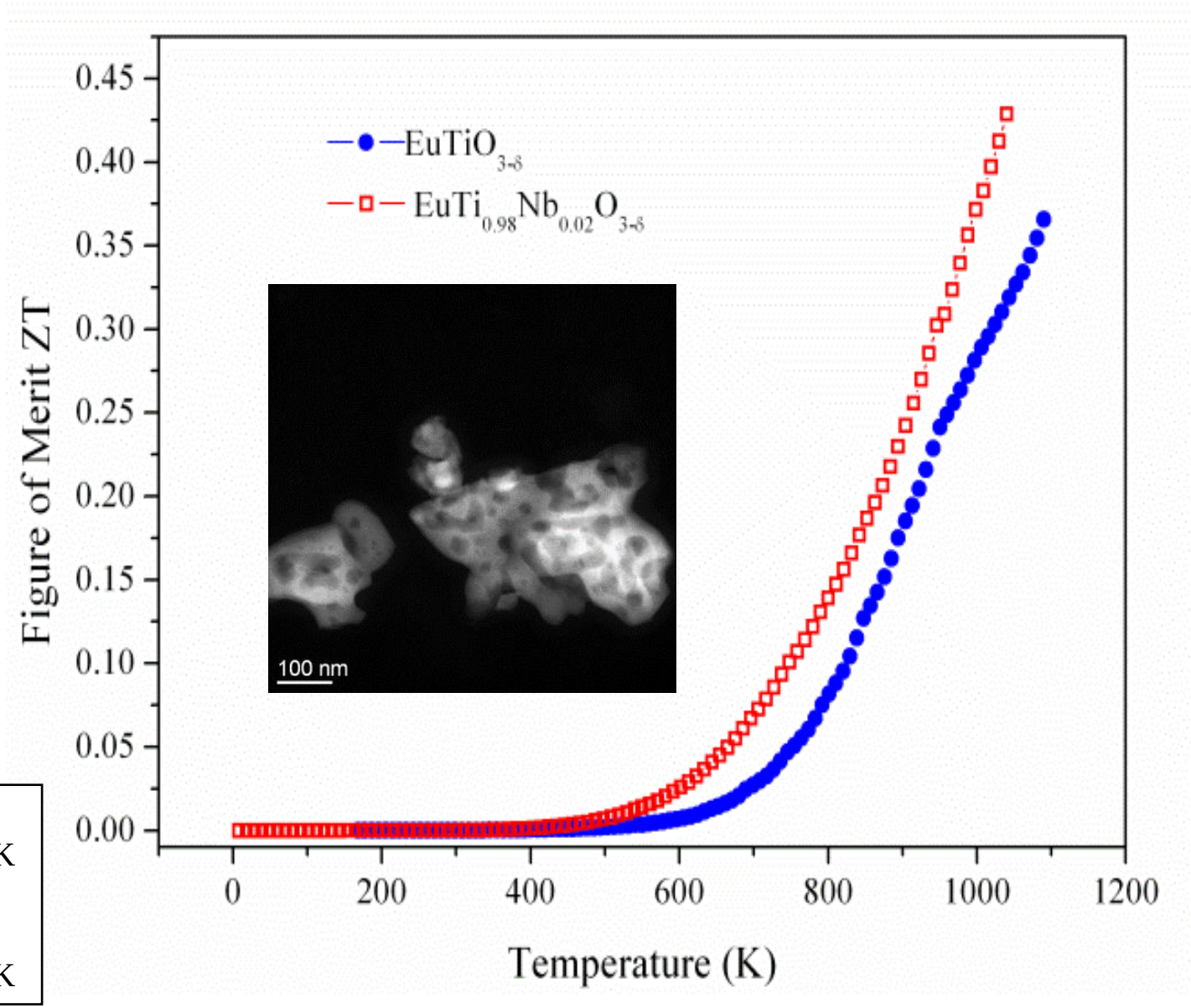

$EuTi_{0.98}Nb_{0.02}O_3$
ZT = 0.43 at T = 1040 K

$EuTiO_3$
ZT = 0.37 at T = 1090 K

$Sr_xLn_{1-x}TiO_{3-\delta}$ Perovskite-type thermoelectric titanates

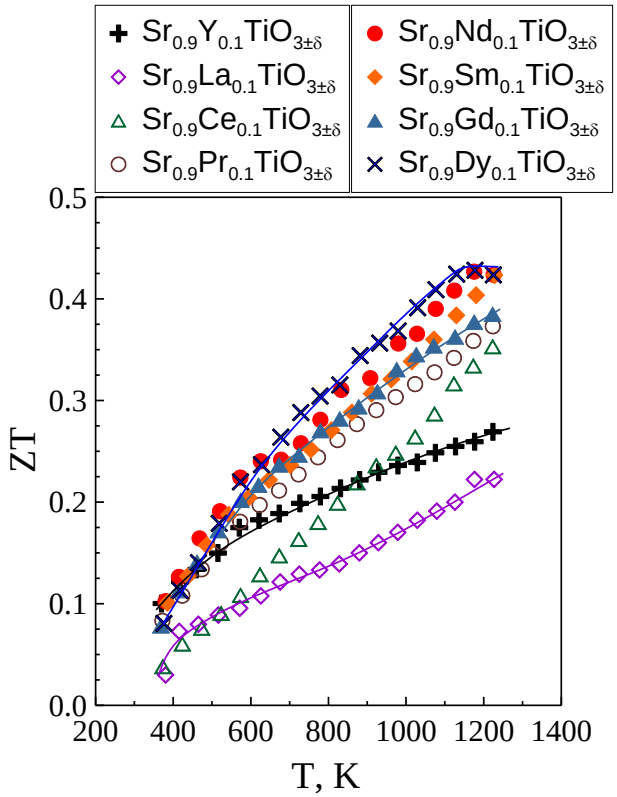

A. V. Kovalevsky, et al , *Phys. Chem. Chem. Phys.*,**16**, (2014) 26946-26954

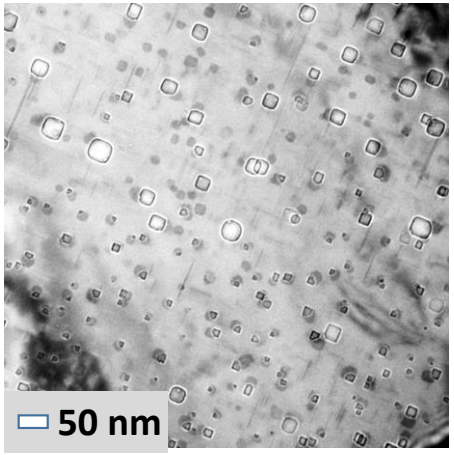

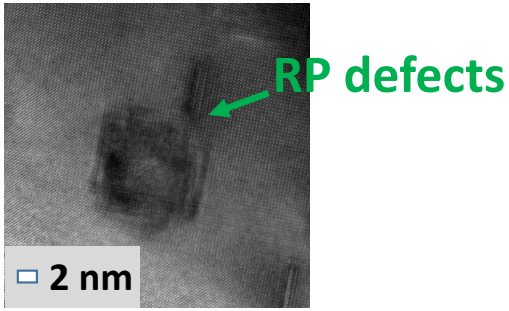

A.Kovalevsky, A. Yaremchenko, M. Aguirre, S. Populoh, S. Patrício, J.Macías, A.Weidenkaff, J.Frade

$BaTiO_3$

Band gap: ~ 3.2 eV

Ferroelectric, piezoelectric, dielectric, thermoelectric,…

$Ba_{1-x}Eu_xTiO_3$

ferromagnetic

Ferroelectric

……

$EuTiO_3$

Band gap: ~ 1 eV

Magnetic, dielectric, incipient ferroelectric, Huge Seebeck,…

Thermoelectric ?

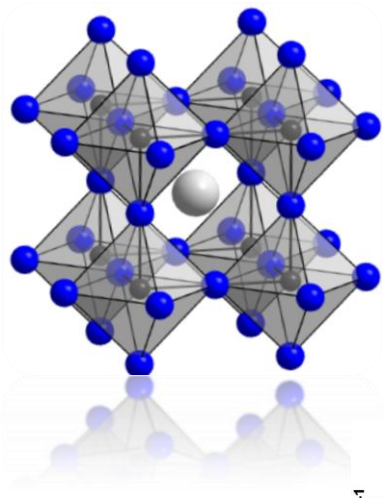

BTO as thermoelectric:

- low electric conductivty
- low lattice thermal conductivity
- abundent elements

ETO as thermoelectric:

- high electric conductiviy
- high lattice thermal conductivity
- rare earth element
- band structure: localised Eu 4f

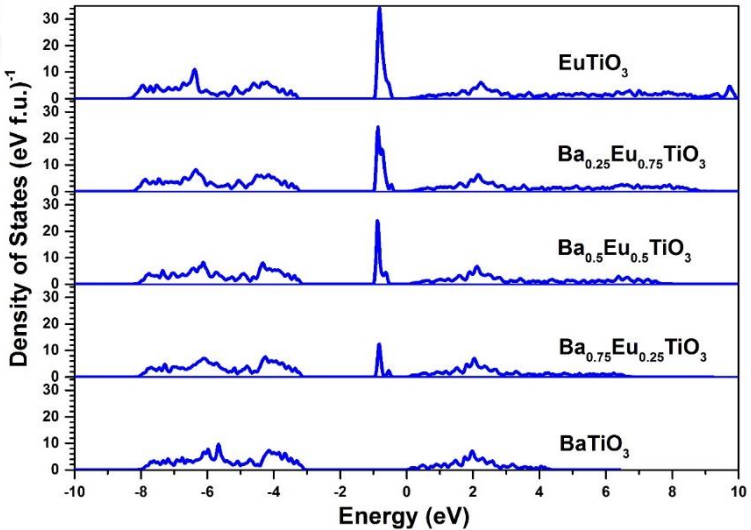

Similarities of BTO & ETO:

- n-type semiconductor
- high Seebeck coefficient
- high temperature stability
- flexible perovskite structure

Synthesis: $Ba_{1-x}Eu_xTiO_3$

Eu_2O_3 dissolves in hot water

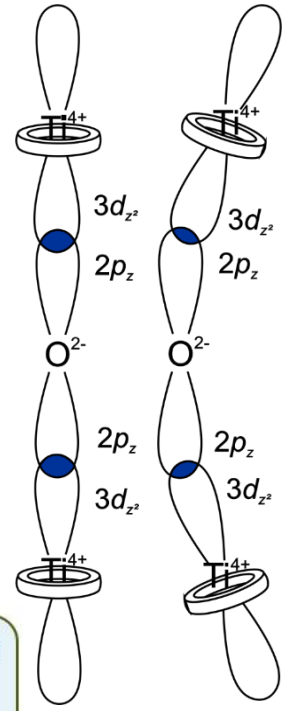

Eu_2O_3, Barium acetate, Citric acid, distilled water

↓

Stirring ~ 30 min at 100 °C

↓

Transparent solution

← **Titanium (IV)bis (ammonium lactato) dihydroxide & Ethylene glycol**

↓

Stirring ~ 2 h at 65 °C

↓

Drying and calcination in air

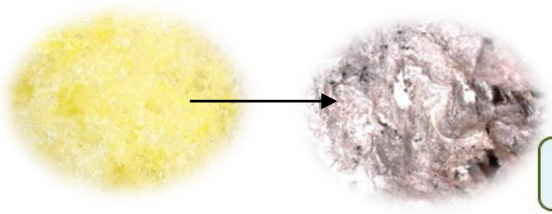

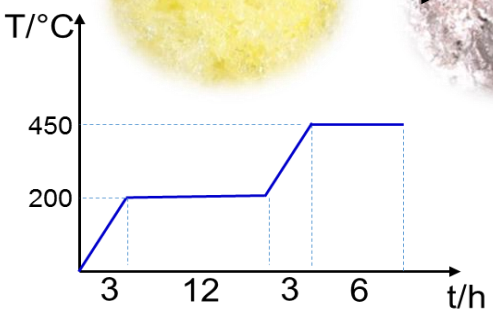

↓

Precursor

Eu^{3+}

↓

Annealing (5% H_2 & 95% Ar)

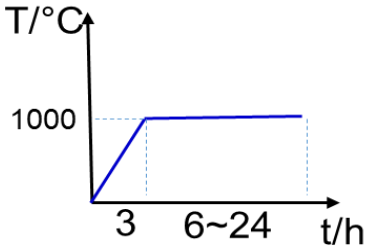

↓

Sample

Eu^{2+}

$Ba_xEu_{1-x}TiO_{3-\delta}$
Unit cell parameters as function of the Eu concentration

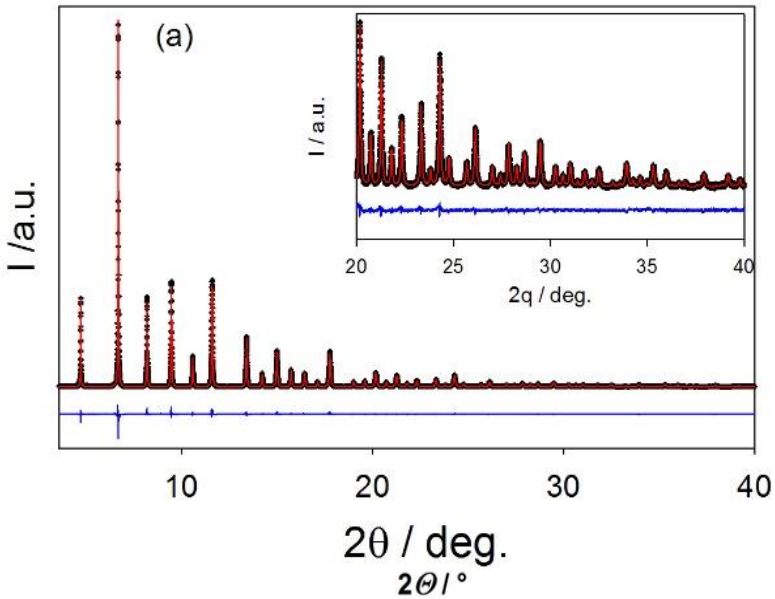

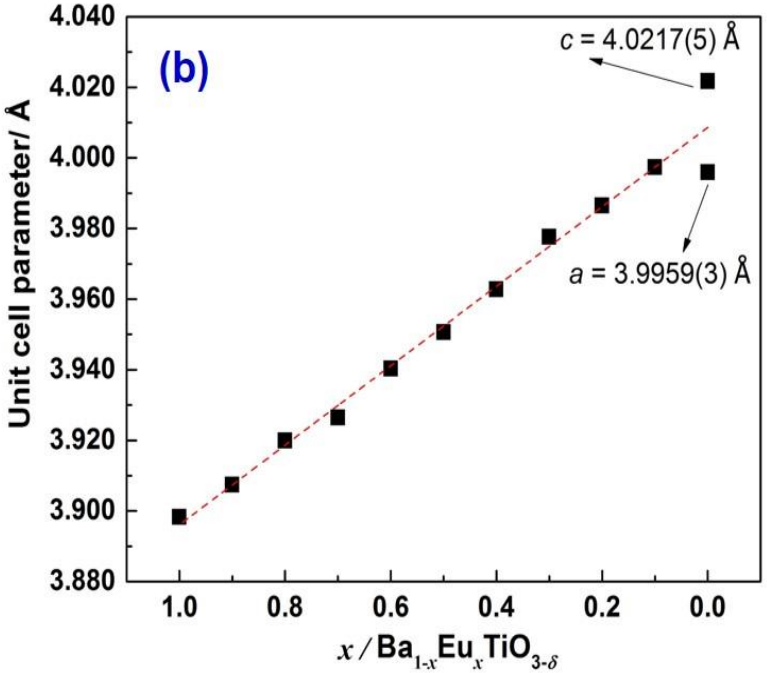

Vegard's law: distances of the nearest-neighbor ions become shorter due to the contraction of the unit cell

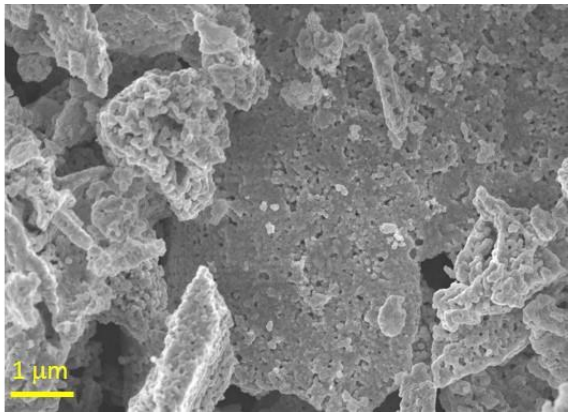

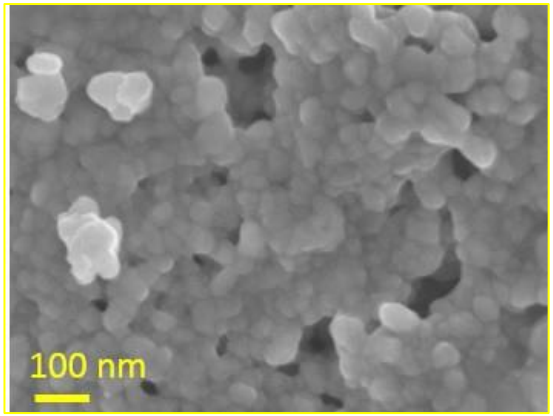

homogeneous morphology with particle size ~ 40 nm.

X. Xiao et al, *PCCP*, in press

Seebeck coefficient of $Ba_{1-x}Eu_xTiO_{3-\delta}$

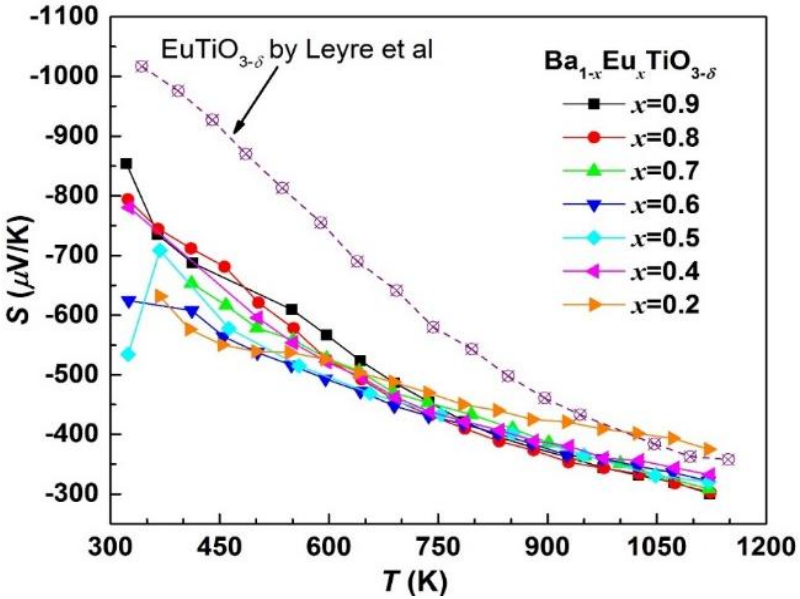

high *T* limit: Heikes formula

$K_B T$ «U_0 on-site repulsion (U_0 = 0.1~1 eV)

$$S(T \to \infty) = \frac{-k_B}{e} \ln \frac{2(1-n)}{n}$$

n = carriers per unit cell

P. M. Chaikin et al. Phys. Rev. B 13, 647 (1976)

- **low temperature: no well-defined relation between Eu content and *S* value;**
- **high temperature (*T* > 1000 K): the |S| value decreases with Eu content.**

Samples No.	$\sigma_{1123\,K}$ (S/m)	E_A (eV)	S_{1123K} (μV/K)	E_s (eV)	W_p (eV)	$n_{1123\,K}$ ($\times 10^{20}$ cm^3)	μ (cm^{2}V^{-1}s^{-1})
x = 0.2	945	0.24	-375	0.18	0.12	4.0	0.15
x = 0.4	1990	0.24	-332	0.23	0.02	6.5	0.19
x = 0.5	2948	0.33	-320	0.30	0.06	7.5	0.25
x = 0.6	3081	0.32	-321	0.24	0.16	7.5	0.26
x = 0.7	4300	0.29	-308	0.34	-	8.7	0.31
x = 0.8	5317	0.26	-302	0.27	-	9.3	0.35
x = 0.9	6289	0.30	-300	0.30	-	9.6	0.41

Electrical conductivity of $Ba_{1-x}Eu_xTiO_{3-\delta}$

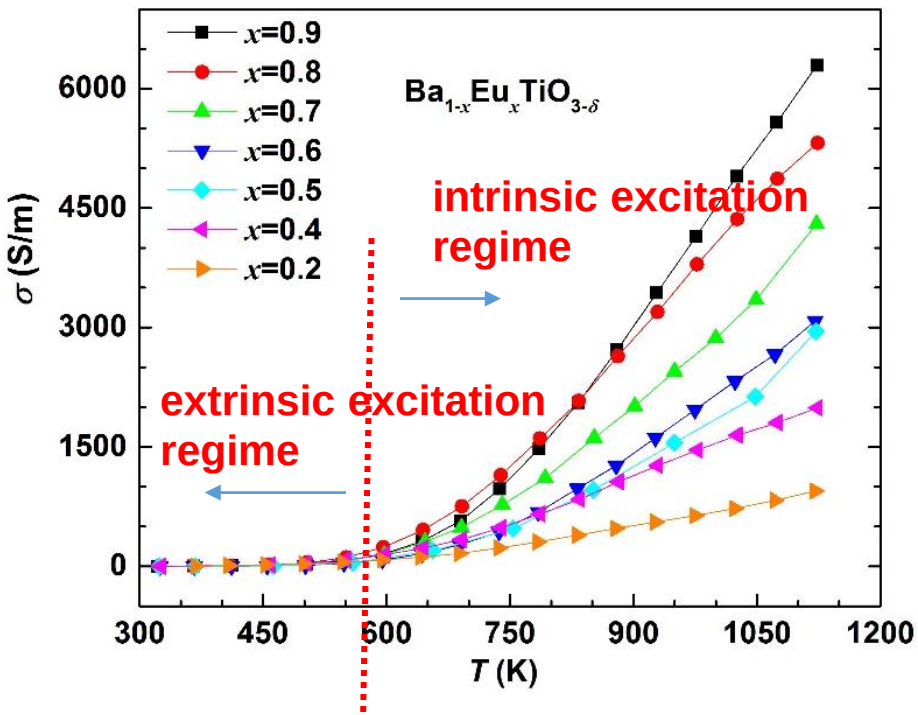

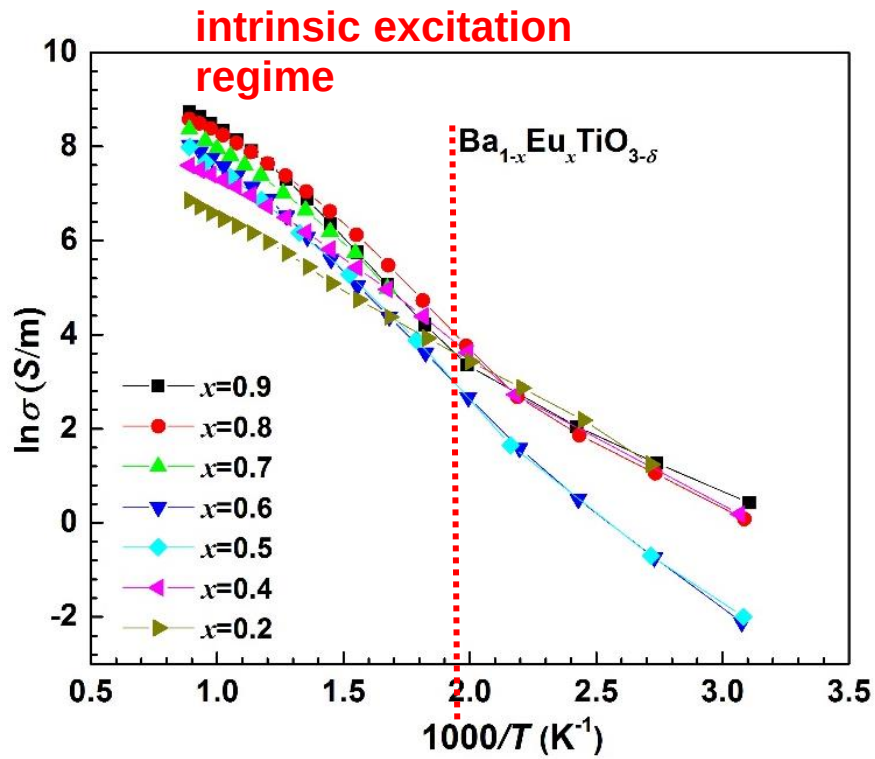

Eu 4f electrons are excited into the conduction band and dominate the electron transport properties at high temperature.

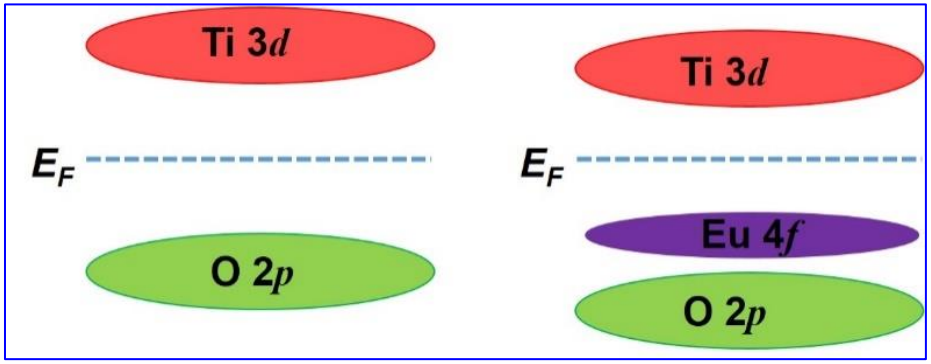

schematic diagram of the band structure of BTO and ETO.

Electron transport mechanism of $Ba_{1-x}Eu_xTiO_{3-\delta}$

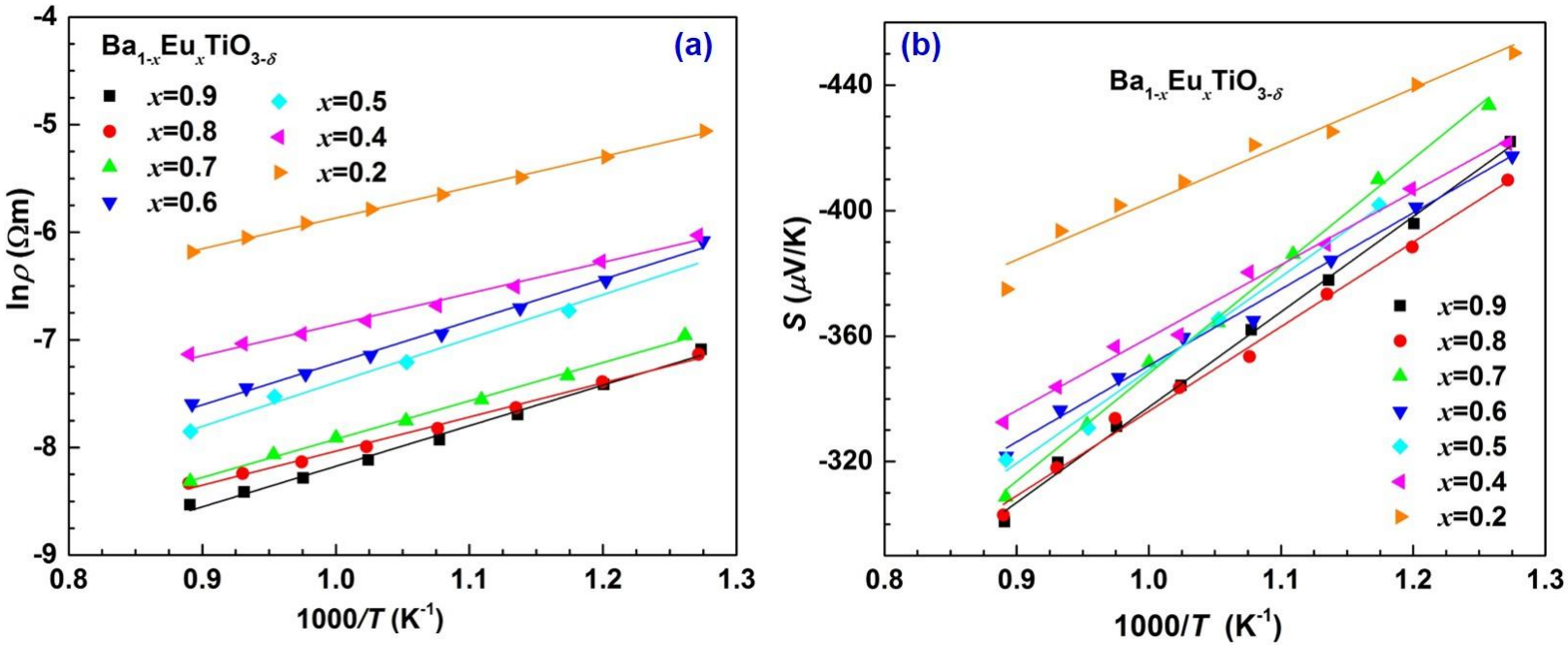

lnρ and *S* as a function of 1000/ T

Arrhenius formula:

$$\rho(T) = \rho_0 \exp\left(\frac{E_A}{k_B T}\right) \longrightarrow E_A$$

Mott's adiabatic small polaron conduction model:

$$S = \frac{k_B}{e}\left(\frac{E_S}{k_B T} + r\right) \longrightarrow E_S$$

$E_A > E_S$: thermally activated hopping

hopping binding energy:

$$W_p = 2(E_A - E_S)$$

Electron transport mechanism of $Ba_{1-x}Eu_xTiO_{3-\delta}$

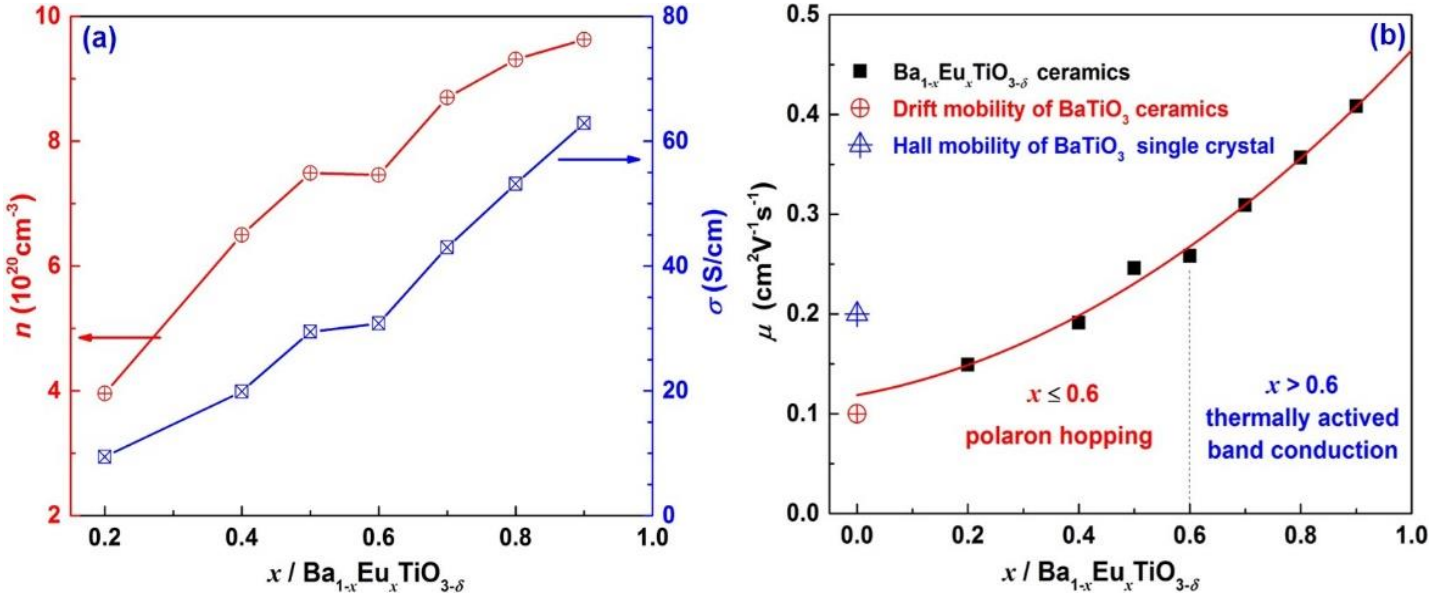

(a) The charge carrier concentration (n), electrical conductivity (σ) and (b) carrier mobility (μ) as a function of Eu-content (x) at 1123 K.

- ***x* ≤ 0.6, $E_A > E_S$ dominated conducting mechanism belongs to polaron hopping conduction.**
- ***x* > 0.6, thermally activated band conduction ?**

Samples No.	$\sigma_{1123\,K}$ (S/m)	E_A (eV)	S_{1123K} (μV/K)	E_s (eV)	W_p (eV)	$n_{1123\,K}$ ($\times 10^{20}$ cm^3)	μ (cm^{2}V^{-1}s^{-1})
x = 0.2	945	0.24	-375	0.18	0.12	4.0	0.15
x = 0.4	1990	0.24	-332	0.23	0.02	6.5	0.19
x = 0.5	2948	0.33	-320	0.30	0.06	7.5	0.25
x = 0.6	3081	0.32	-321	0.24	0.16	7.5	0.26
x = 0.7	4300	0.29	-308	0.34	-	8.7	0.31
x = 0.8	5317	0.26	-302	0.27	-	9.3	0.35
x = 0.9	6289	0.30	-300	0.30	-	9.6	0.41

Thermal conductivity of $Ba_{1-x}Eu_xTiO_{3-\delta}$

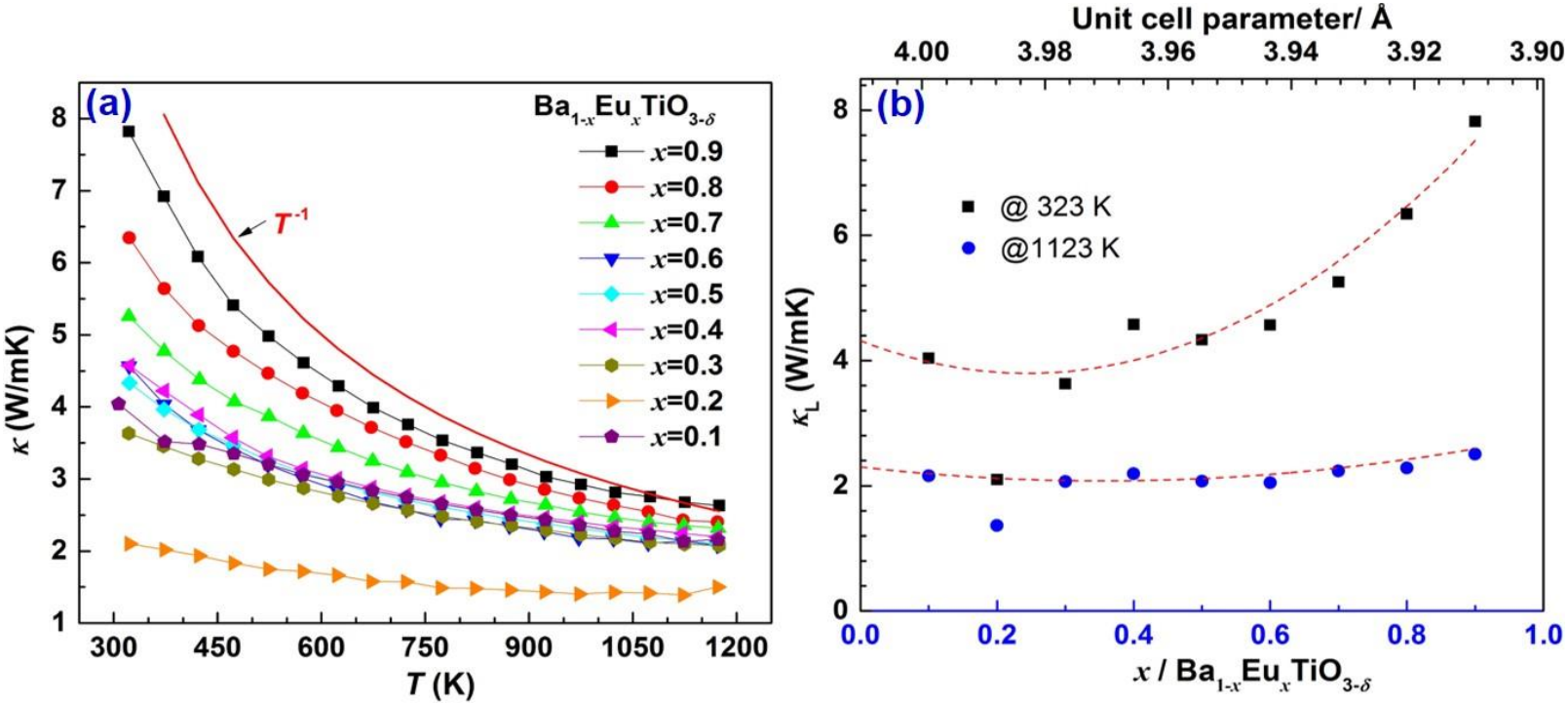

- κ follows a T^{-1} dependence, indicating the dominant phonon scattering mechanism is the Umklapp scattering (phonon–phonon interactions).
- Eu substitution decreases the Ti–O distance, strengthening the Ti–O bond, resulting in higher κ_L.
- In this studied system, the changes in the bond strength appear to be more effective for depressing the thermal conductivity than the simultaneously occurring point defect scattering.

Hiroaki Muta∗, Ken Kurosaki, Shinsuke Yamanaka,J ournal of Alloys and Compounds 368 (2004) 22–24

Power factor & *ZT* value of $Ba_{1-x}Eu_xTiO_{3-\delta}$

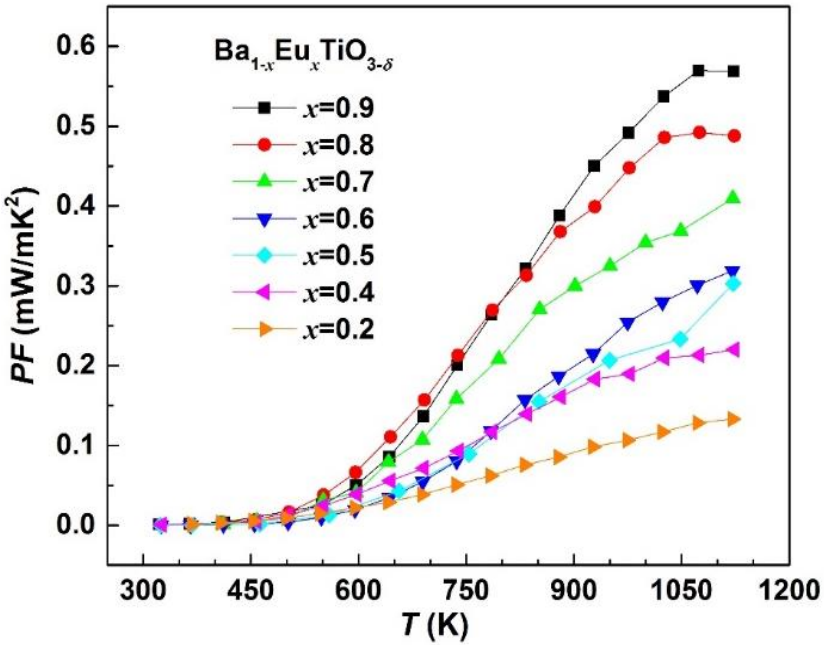

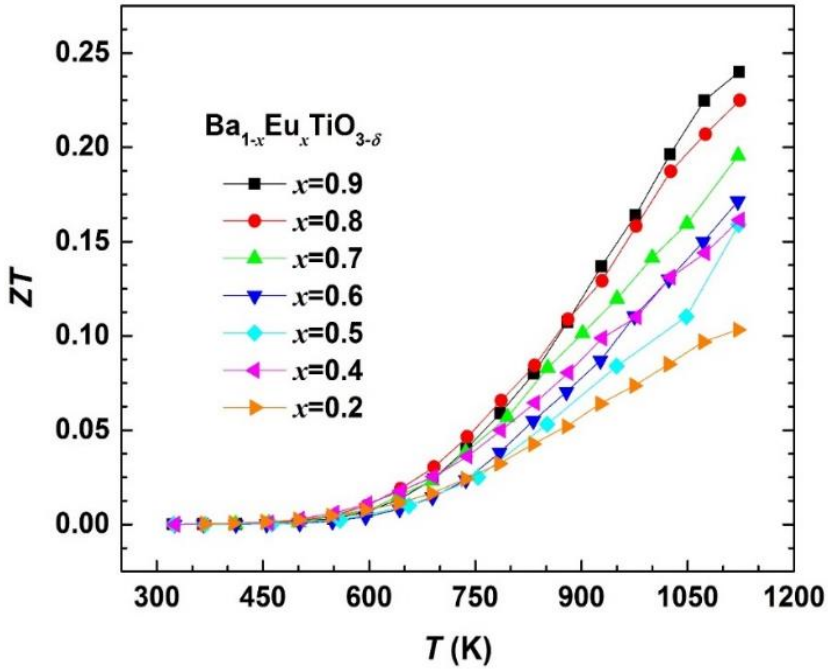

- **Eu substitution significantly enhances the *Power factor* and the *ZT value*, resulting from that Eu substitution causes a particularly strong improvement in electrical conductivity.**
- **$Eu_{0.9}Ba_{0.1}TiO_3$ *ZT* = 0.24 at 1122 K**

Intermetallics: half-Heusler compounds

n-type TiNiSn, p-type TiCoSb

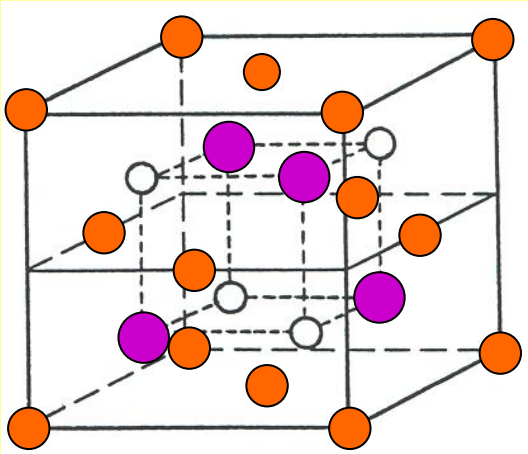

M=Ti, Zr, Hf

Ni/Co

Sn/Sb

Four fcc sublattices shifted ¼ along (111).
A (0,0,0) occupied by Ni/Co
B (¼, ¼,¼) occupied by M
C (¾,¾,¾) occupied by Sn/Sb

narrow bands
high effective mass
a large Seebeck coefficient

high thermal conductivity
TiNiSn: ~10-20 W/mK
commercial Bi_2Te_3: ~1-2 W/mK

Properties and functions of Heusler compounds

Permanent magnets

Multiferroics

Piezoelectrics

Thermoelectrics

Photovoltaics

p-type transparent conductors

Superconductors

Topological insulators

…

TE-HH: Synthesis methods

$(Ti_{0.2}Hf_{0.8})Co_{1-x}Mn_xSb \quad (0 < x < 0.16)$

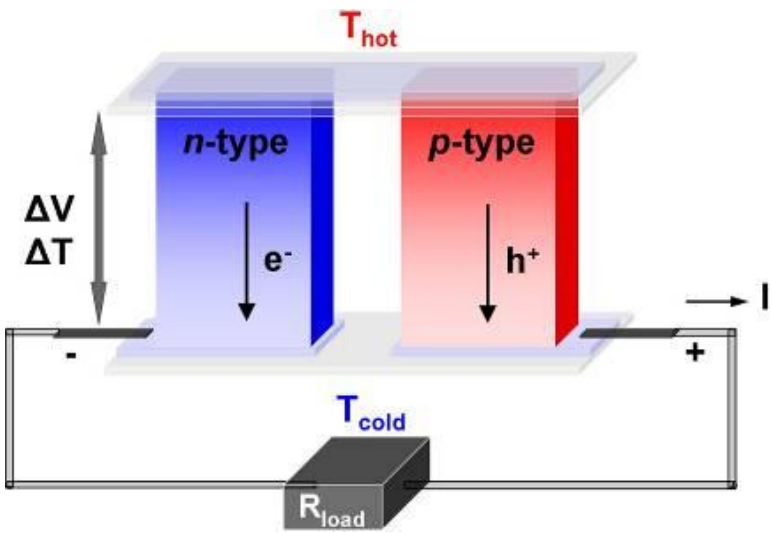

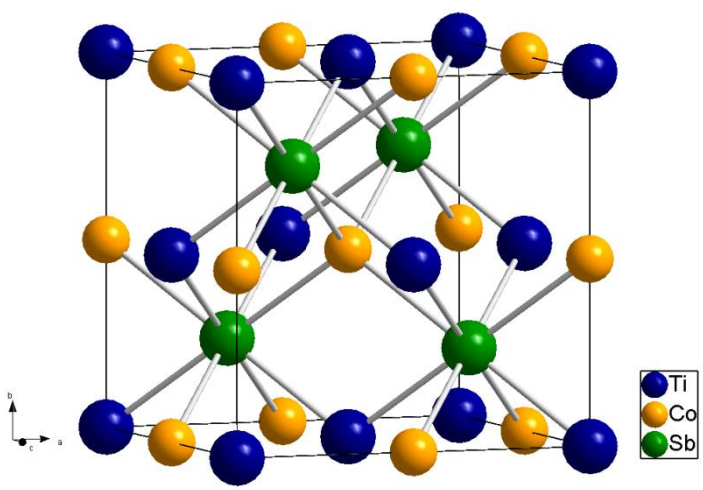

Mixing metals/Arc melting/annealing

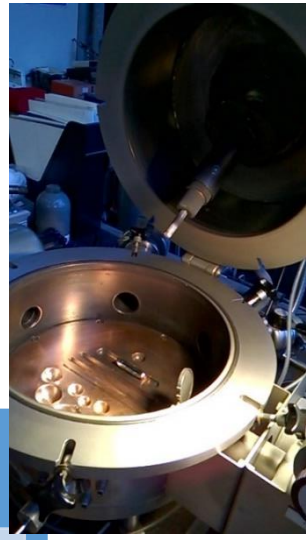

Induction/MW melting

SPS

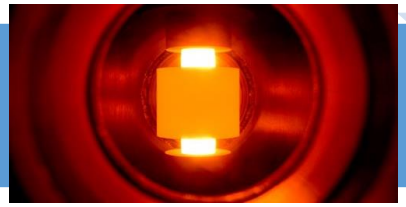

Polishing

Cutting

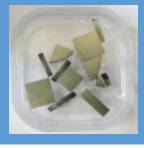

XRD : $Zr_{0.43}Hf_{0.57}NiSn$

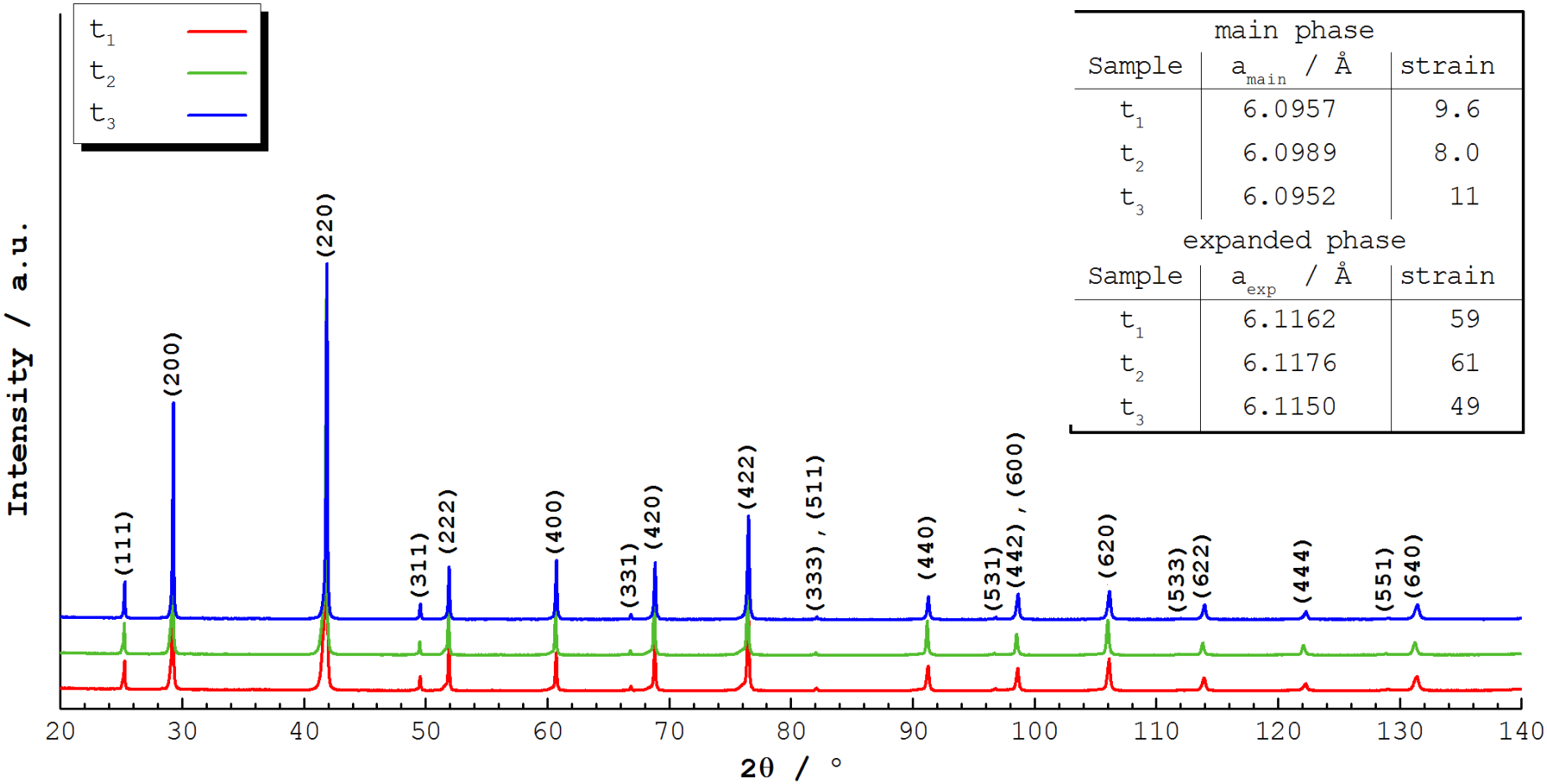

main phase		
Sample	a_{main} / Å	strain
t_1	6.0957	9.6
t_2	6.0989	8.0
t_3	6.0952	11
expanded phase		
Sample	a_{exp} / Å	strain
t_1	6.1162	59
t_2	6.1176	61
t_3	6.1150	49

- Diffusion t_1 = 8 min, t_2 = 32 min; t_3 = 72 min
- Main phase: half-Heusler
- Expanded phase with the same symmetry.

Electrical resistivity of $Zr_{0.43}Hf_{0.57}NiSn$

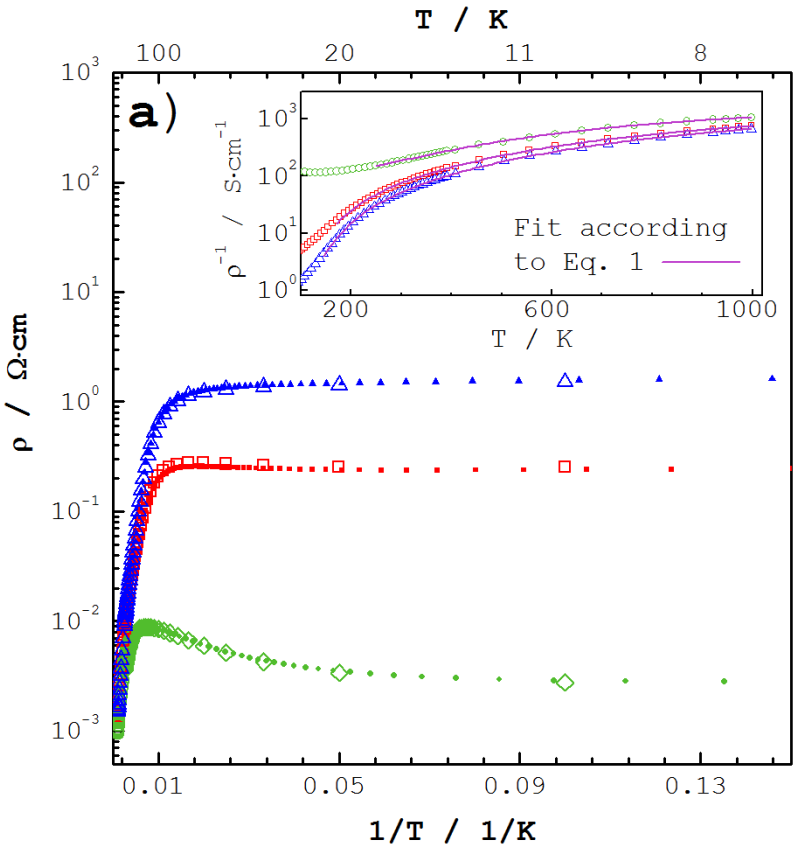

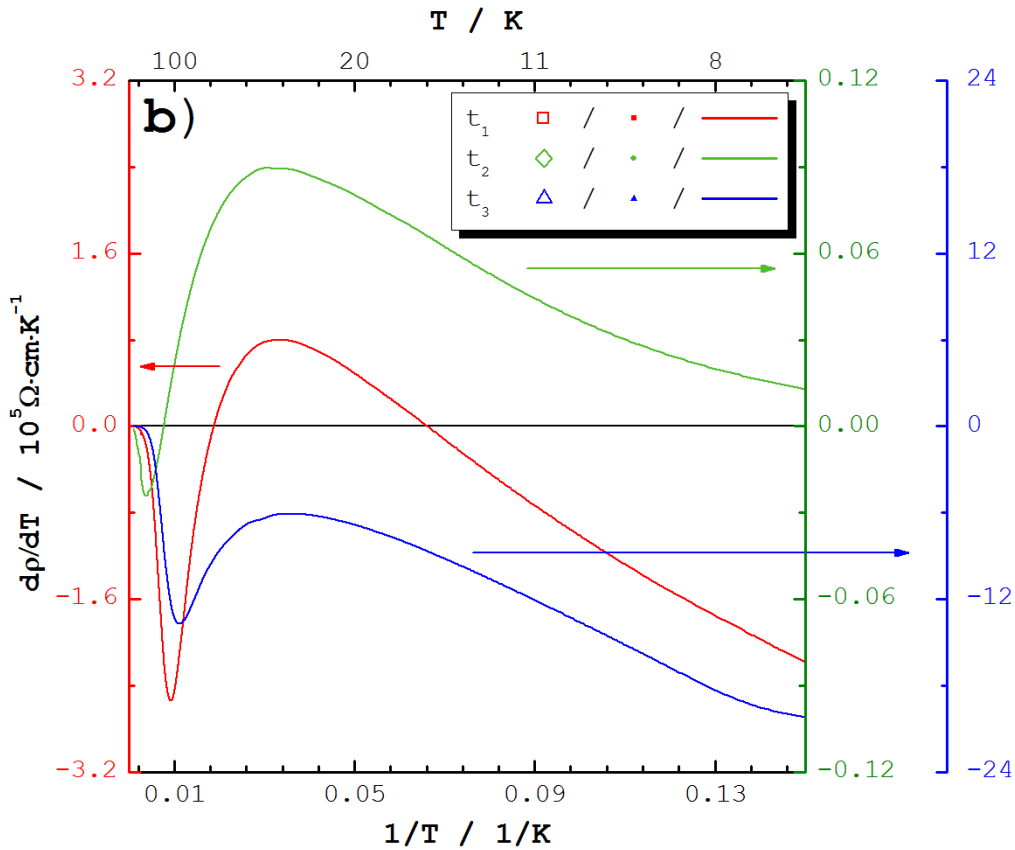

	Sample		
Parameters	t_1	t_2	t_3
T range (K)	170 – 998	250 – 998	145 – 998
ΔE_0 (meV)	330 ± 8	233 ± 6	349 ± 5
ΔE_1 (meV)	108 ± 2	26 ± 2	118 ± 1

- Intrinsic behaviour at high-T
- Presence of an impurity level
- Metallic behaviour at low-*T*

Half-Heusler phases defect control: $Ti_{0.37}Zr_{0.37}Hf_{0.26}NiSn$

- impurity band merge with conduction band.
- modification of the DOS near the edge of the conduction band enhance charge carrier concentration

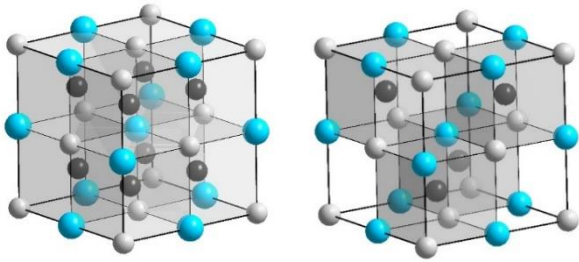

Half-Heusler (XYZ)

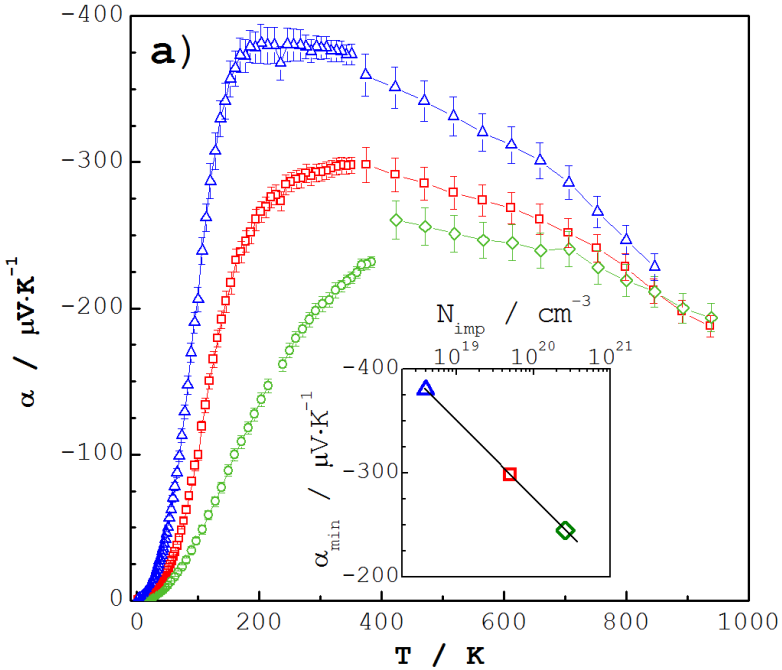

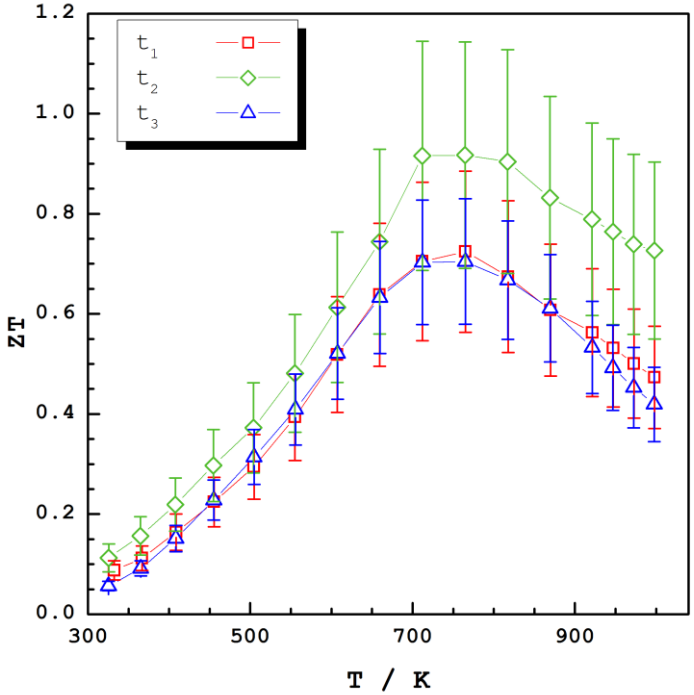

Interstitial Ni defects act as classical dopants – control of *n*

K. Galatzka et al, in preparation

FH nanoprecipitates in HH matrix

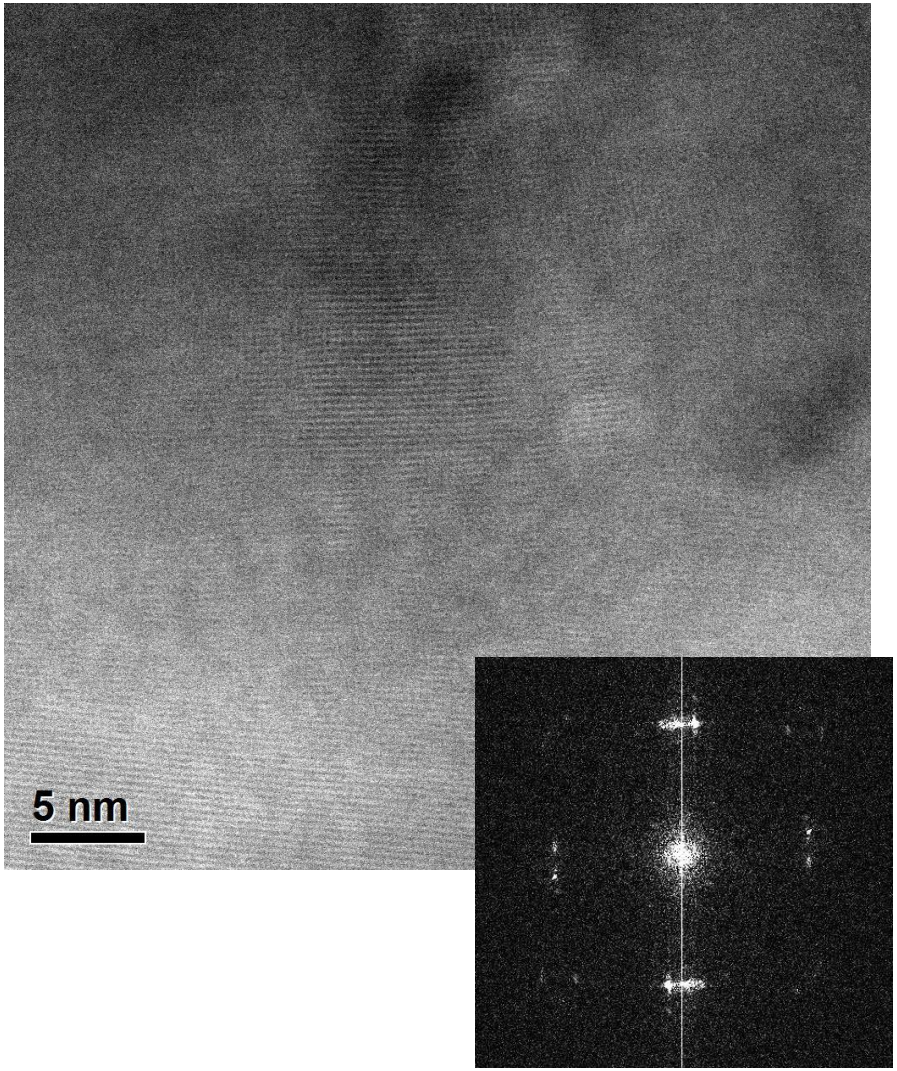

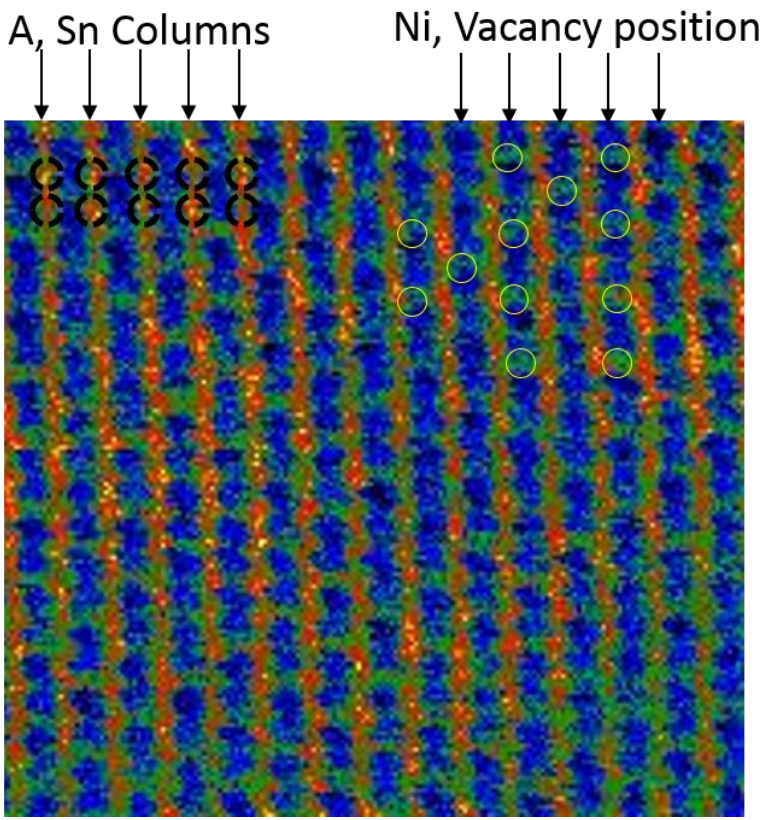

HRSTEM with HAADF in aberration corrected TEM (Titan G3 at 300 keV) by Myriam Aguirre, Zaragoza

K. Galatzka, S. Populoh, MH Aguirre, W. Xie et al, in preparation

Summary and Conclusions

New materials :

- ✓ band gap and defect control by innovative synthesis processes
- ✓ large thermopower in correlated electronic systems
  - ➢ Giant Seebeck in $EuTiO_3$ (S>1000 μV/K)
- ✓ low thermal conductivity by hindering phonon transp. on grain boundaries
  - ➢ synthesis method for titanate nanocubes and foams
- ✓ thermoelectric conversion at T > 700°C in air demonstrated
  - ➢ high T thermoelectric conversion: power output improved 10 times

Acknowledgements

Collaborations: Ryoji Funahashi, Andrei Kovalevski, Jiri Heijtmanek, Joachim Maier, Aldo Steinfeld, ...

Funding: DfG, BmBF, BW, SNF, Vector

Beamtime: ESRF, SINQ

$Zr_{0.4}Hf_{0.6-x}Ta_xNiSn$ Half-Heusler Compounds

reduce Hf content

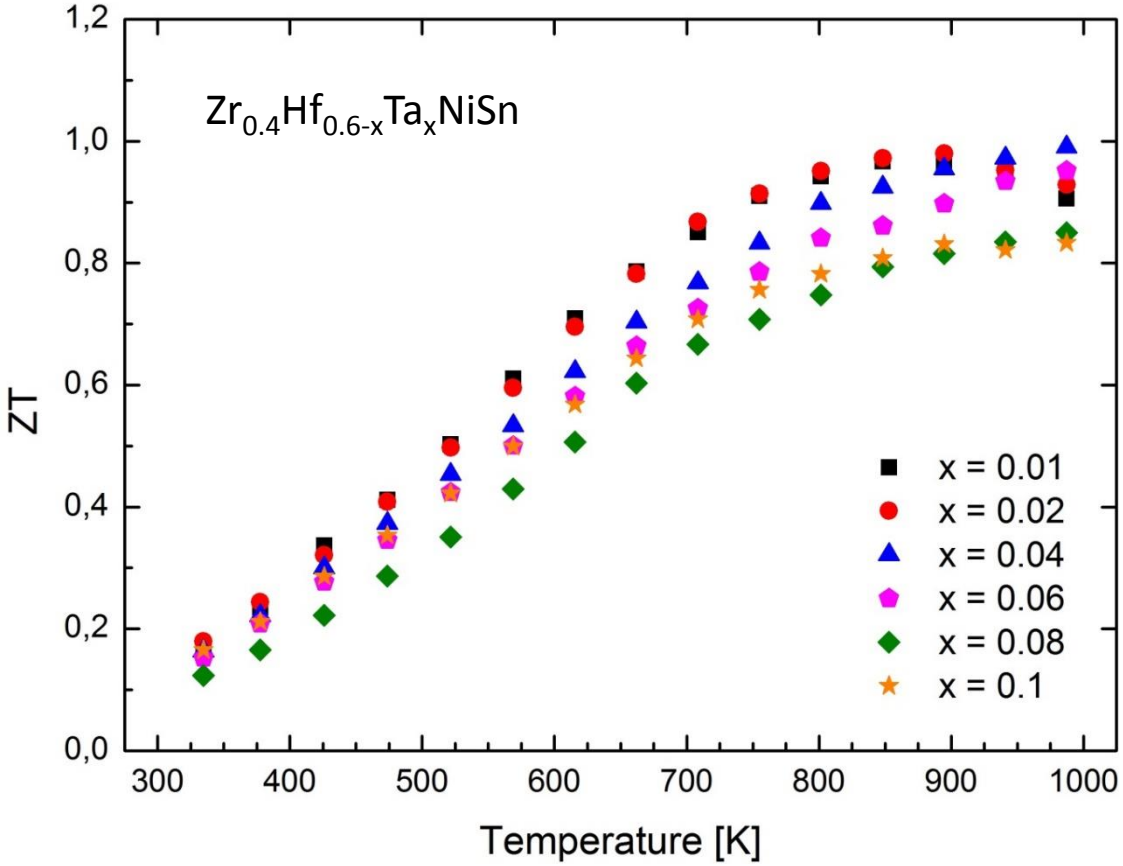

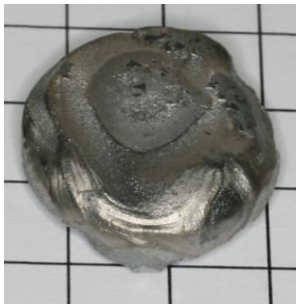

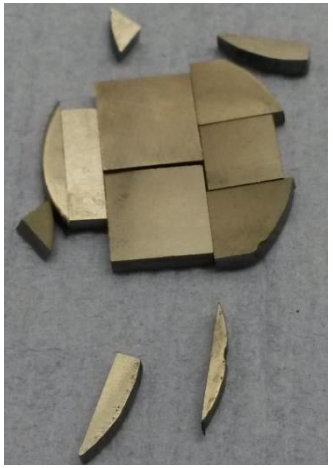

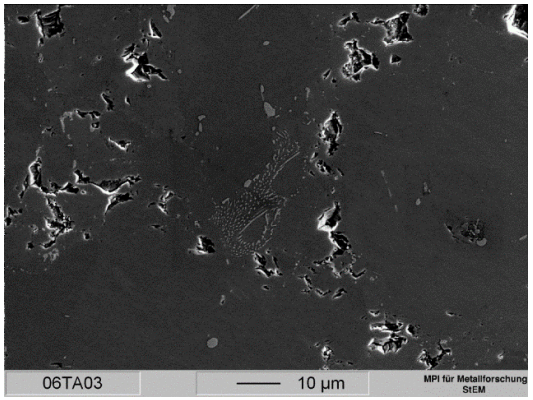

David Wanasuria et al, in preparation

Full Heusler/Half Heusler compounds

T. Graf et al., Prog. Solid State Chem., vol. 39, pp. 1–50, 2011

Heusler structure, $Fm\bar{3}m$ symmetry <-> Half-Heusler structure, $F\bar{4}3m$ symmetry

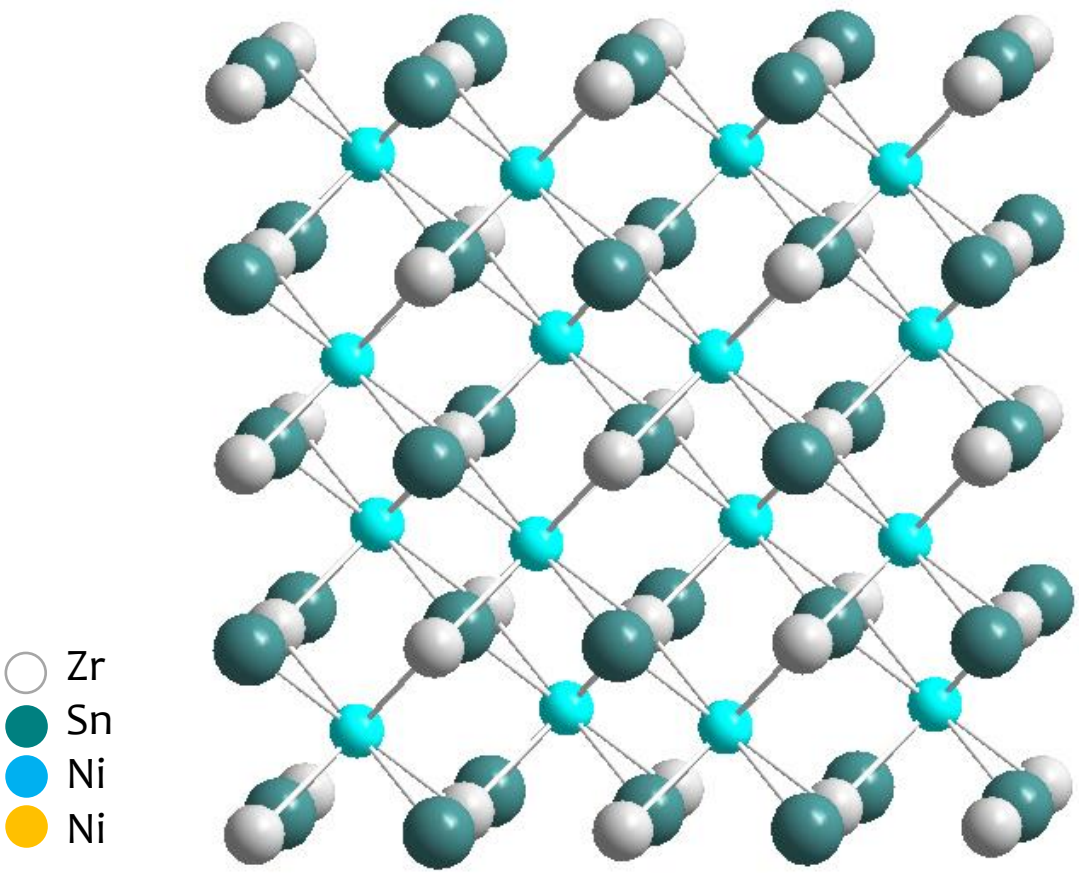

XYZ

Removing 4a Ni atoms per unit cell = change of symmetry

$Sr_xLn_{1-x}TiO_{3-\delta}$

- $EuTiO_3$: Sr for Eu substitution up to x = 0.75 has no detrimental effect on the TE properties
- strong hybridization of the localized Eu *4f* states with the delocalized Ti *3d* states
- reduced titanates possess up to 5 orders of magnitude lower electrical resistivity, confirming that oxygen vacancies act as electron donors
- Soft chemistry synthesis method for nanostructured titanates
  κ from >7 W K^{-1} m^{-1} to <2.5 W K^{-1} m^{-1}

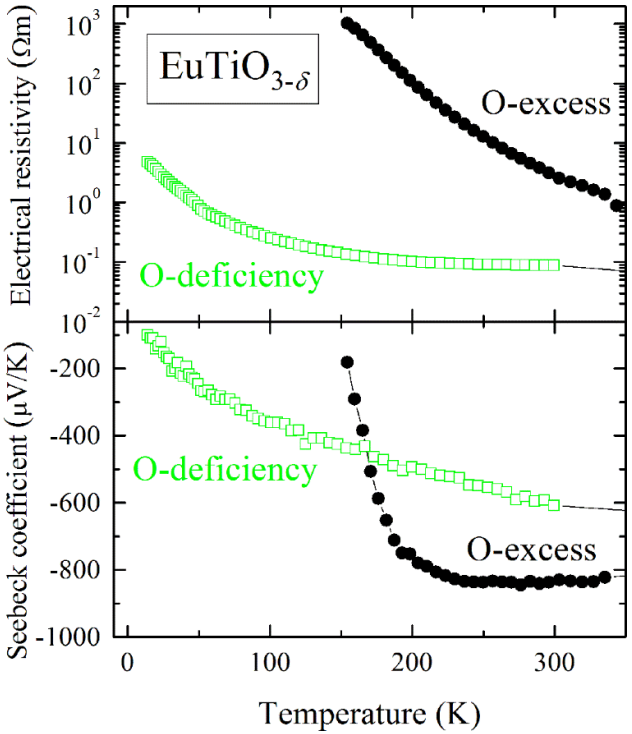

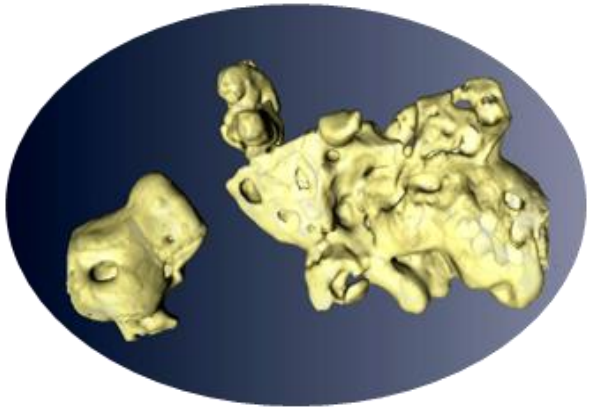

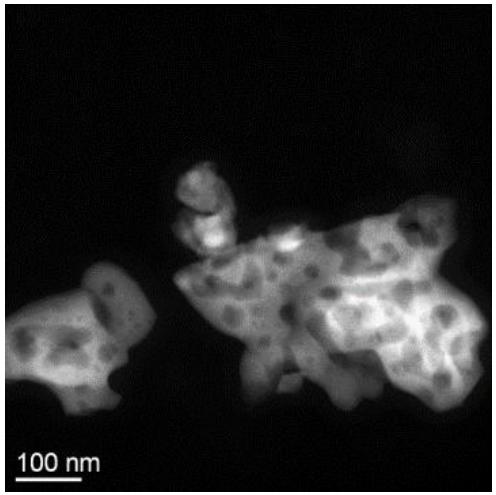

Oxygen content of titanates

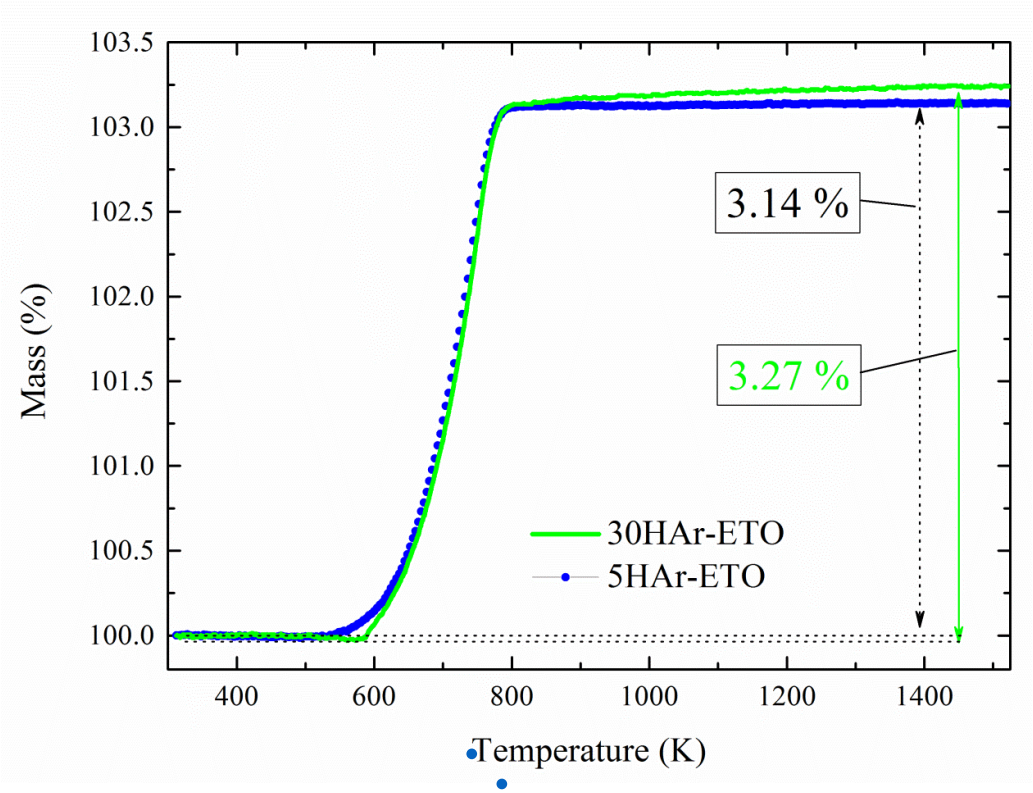

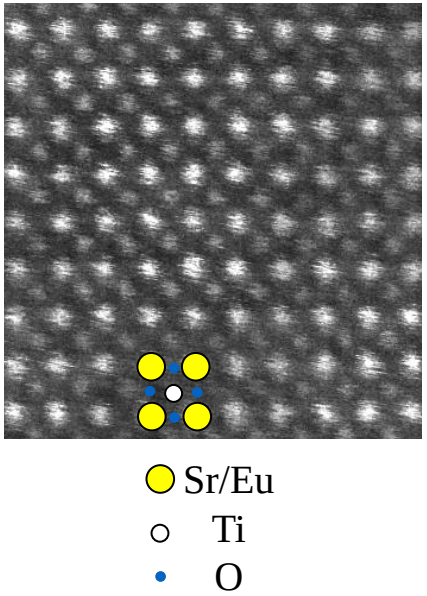

30HAr-ETO: δ = 0.007(5) $EuTiO_{2.993(5)}$ slight O-deficiency
5HAr-ETO: δ = -0.013(3) $EuTiO_{3.013(3)}$ slight O-excess

$Eu_{1-x}Ca_xTi(O,N)_{3\pm\delta}$

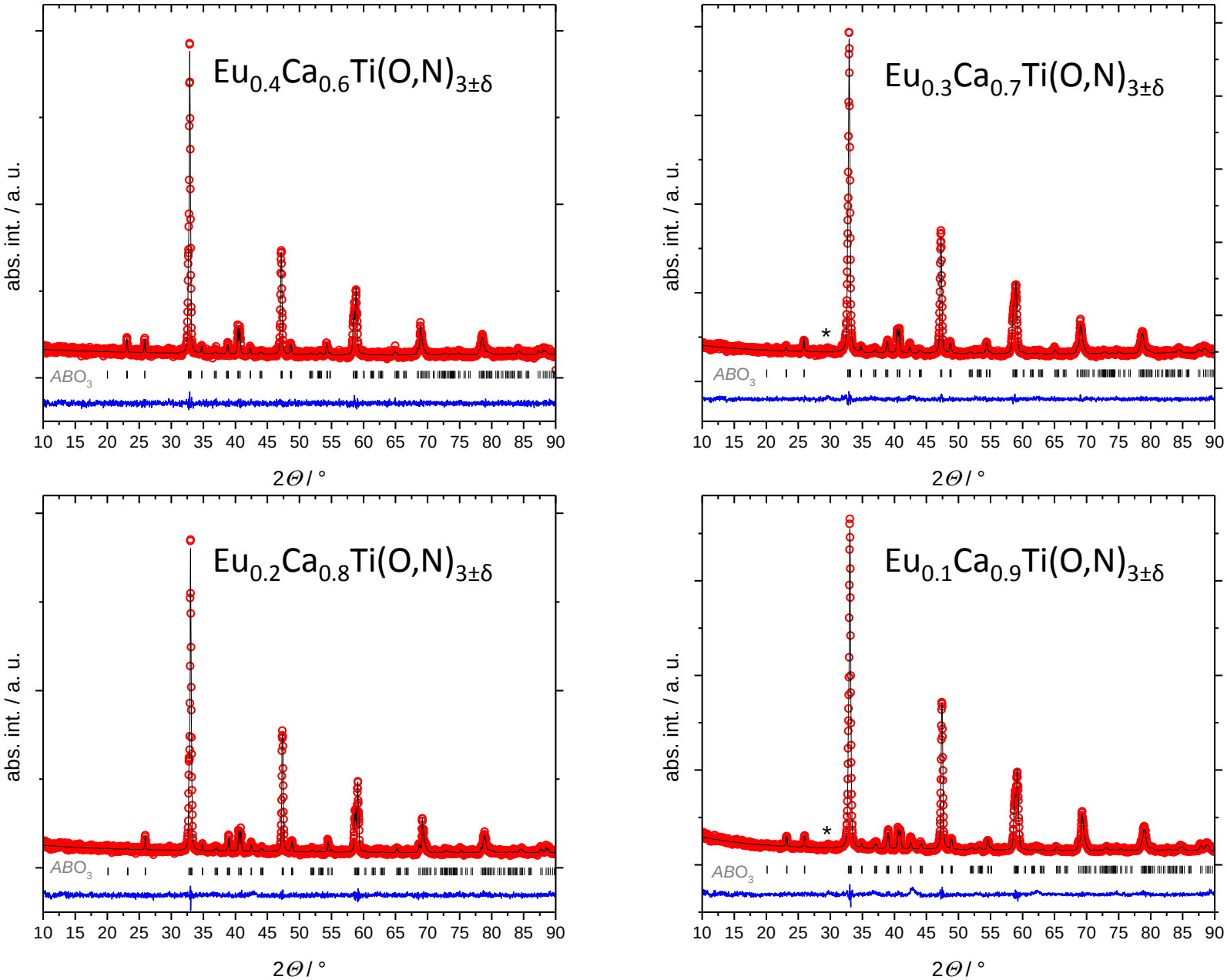

X-ray Photoelectron Spectroscopy (XPS)

Ti 2*p* **$Sr_xEu_{1-x}TiO_{3-\delta}$** Eu 3*d*

30HAr: small content of Ti^{3+}

5HAr: larger content of Eu^{3+} than 30HAr

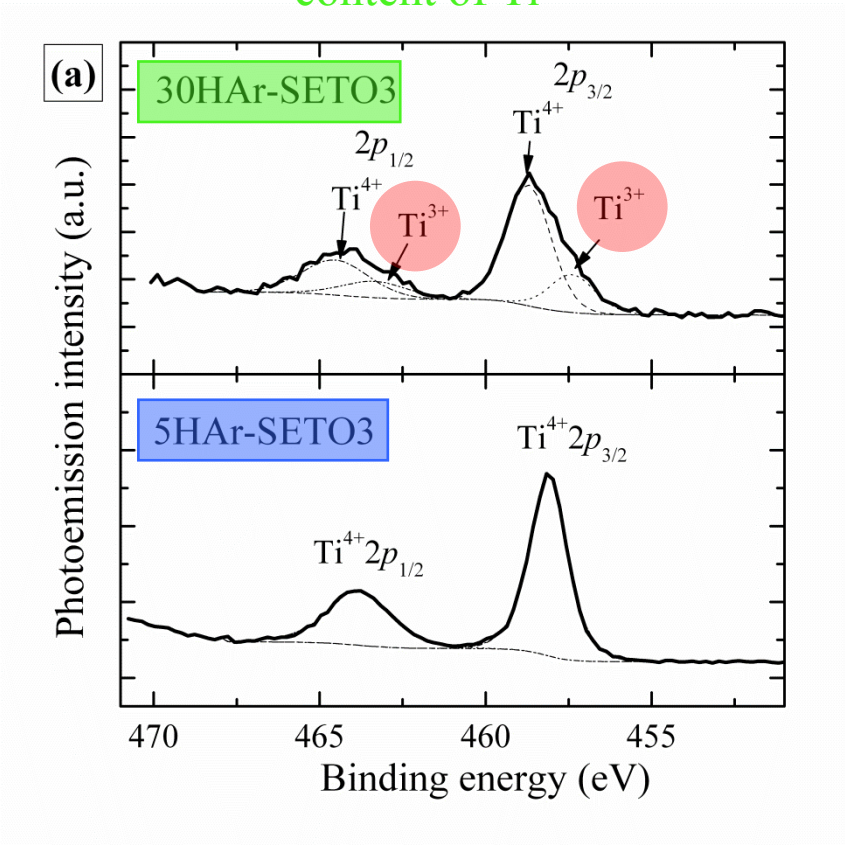

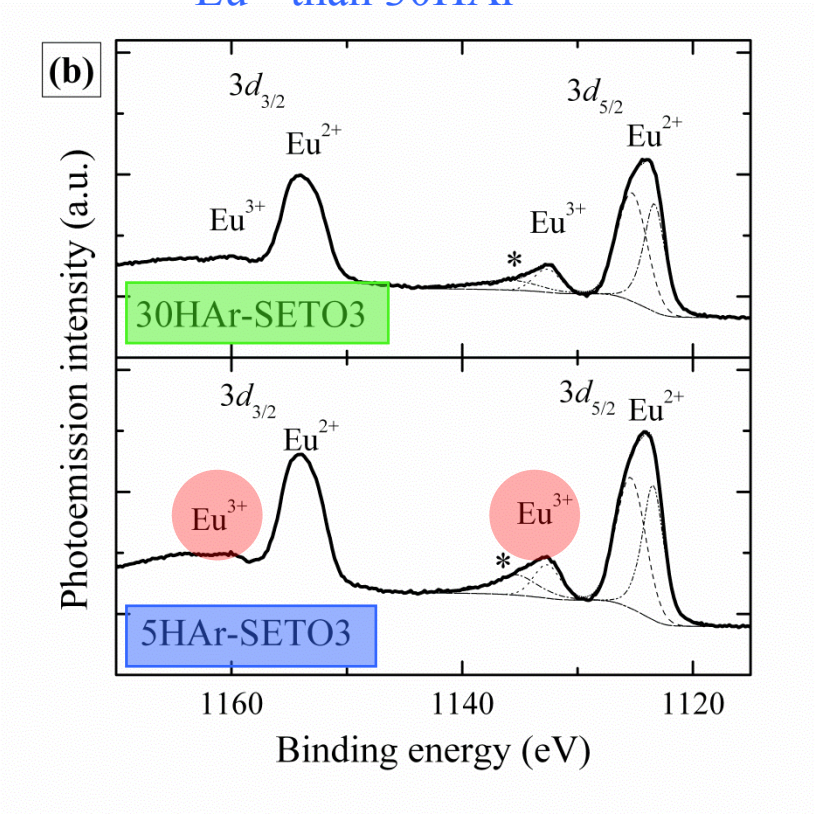

Ratio: Eu^{3+}/Eu^{2+}

$Ba_xEu_{1-x}TiO_{3-\delta}$

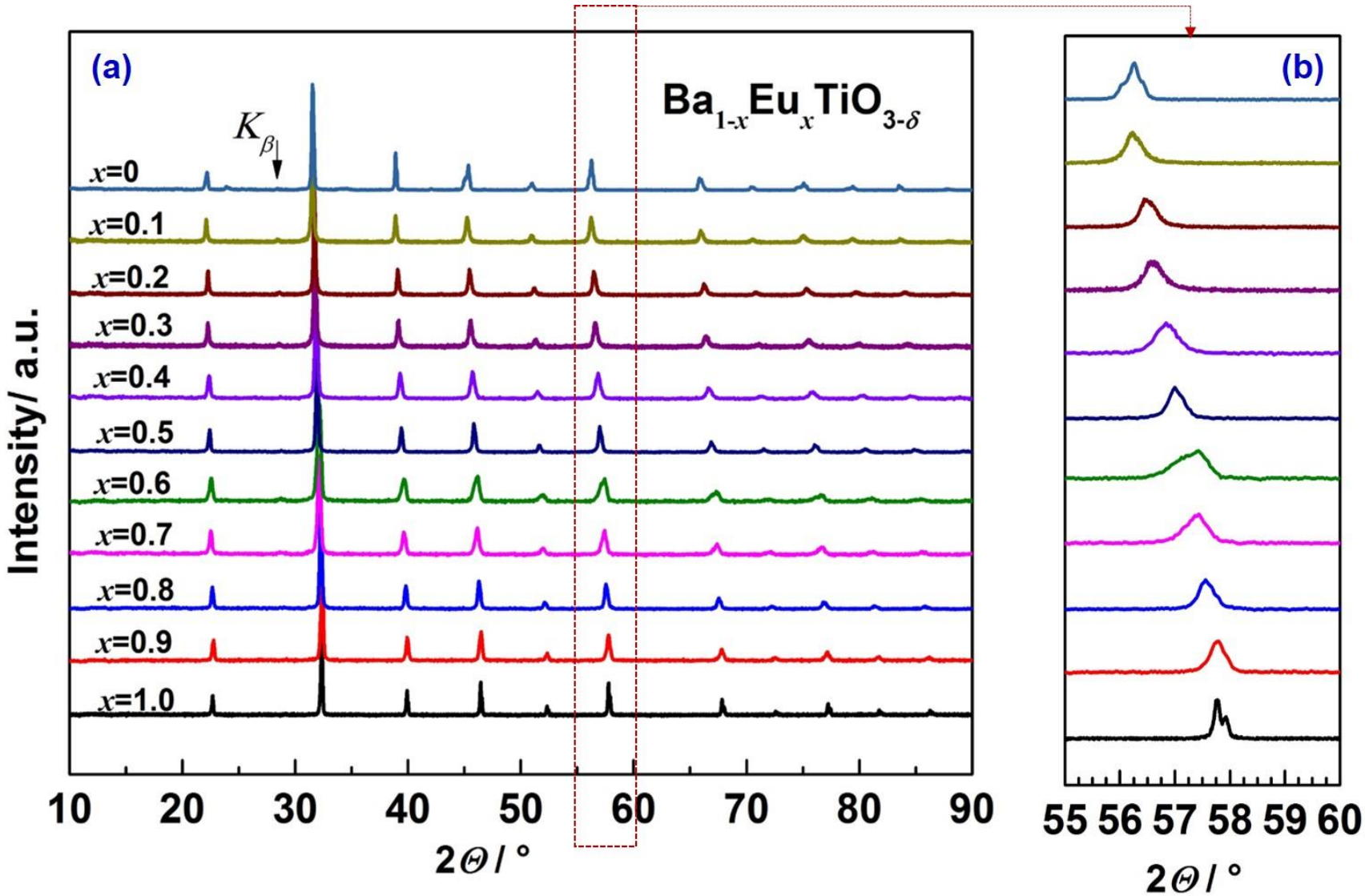

Xingxing Xiao, et al submitted

Multi-sized titanate particles

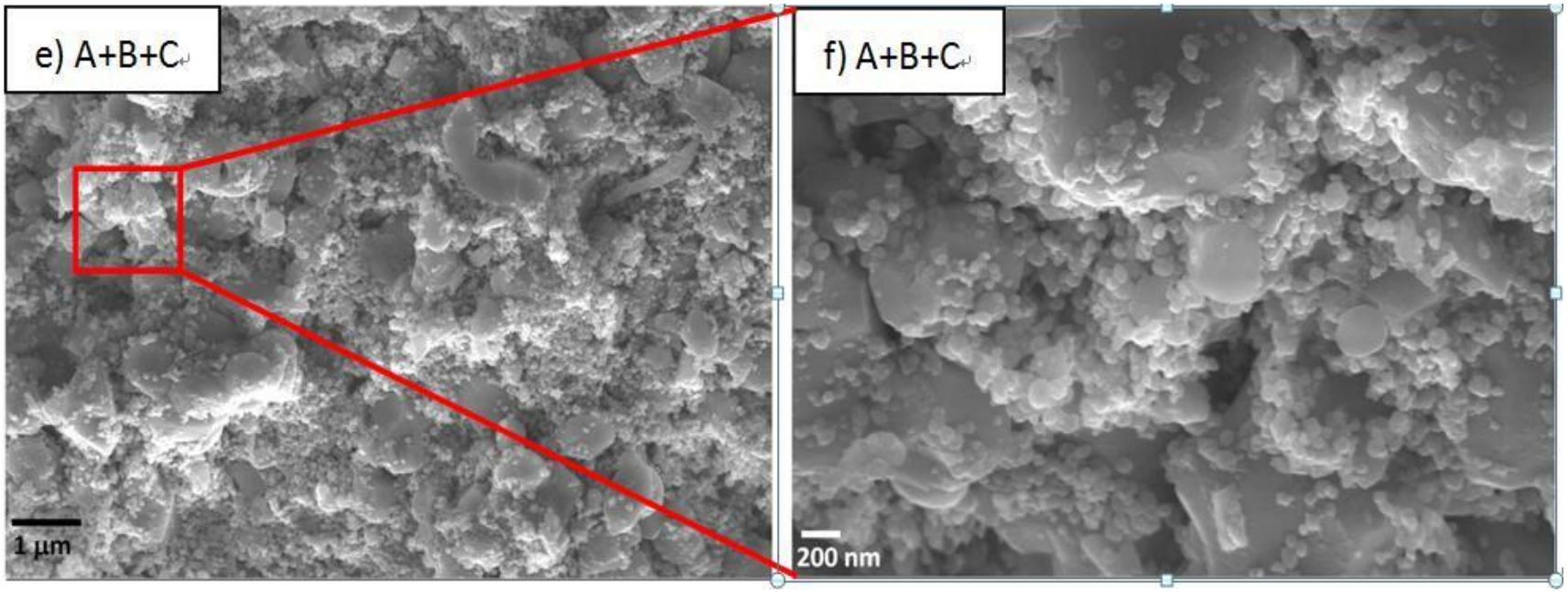

A+B+C	5 µm+500 nm +50 nm

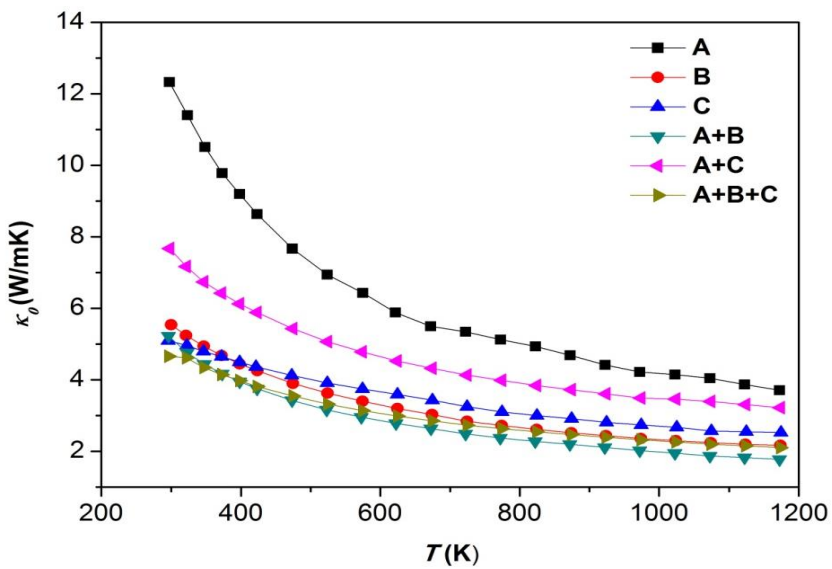

Jingqing Jiang, et al

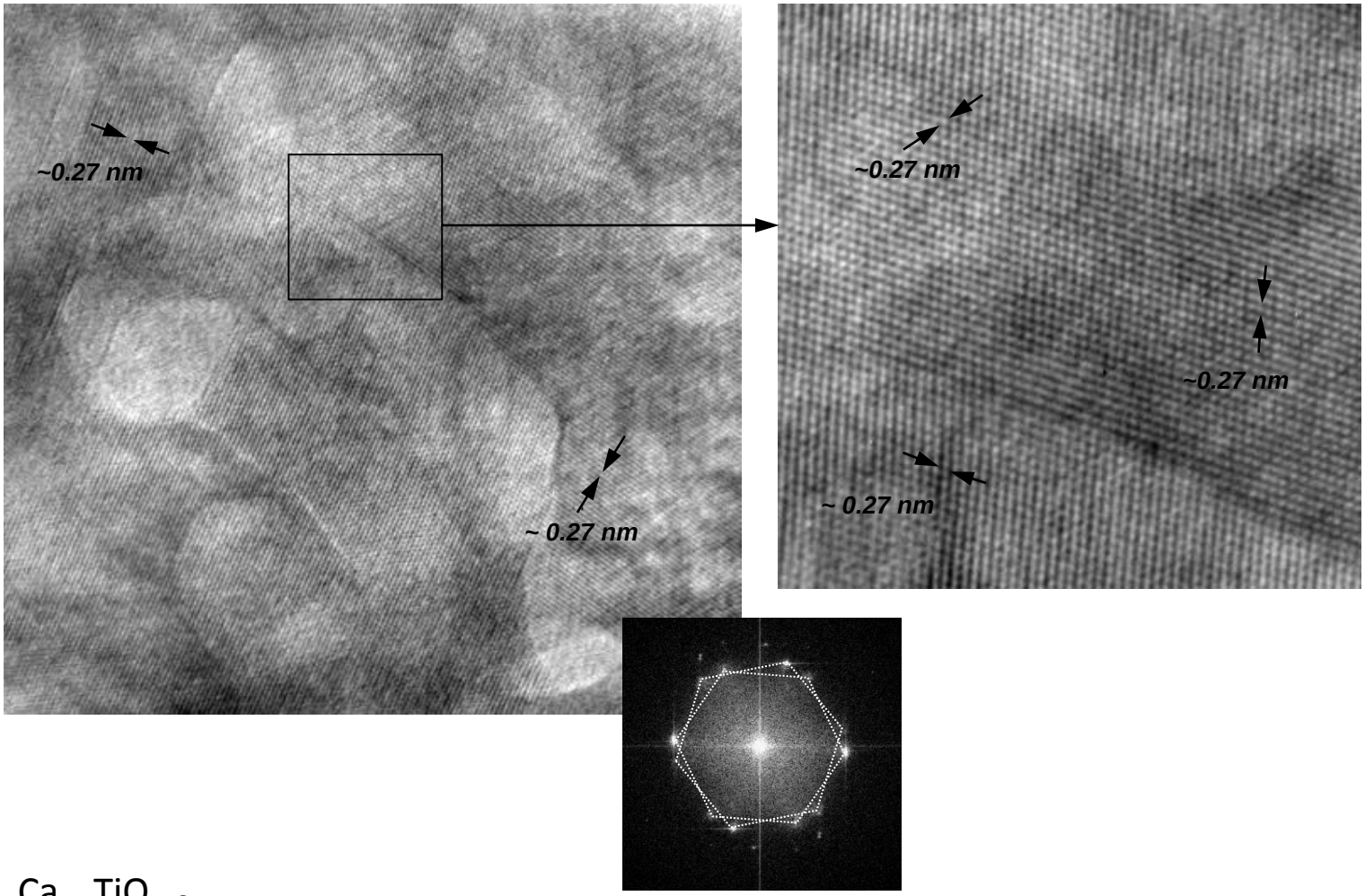

$La_{0.3}Ca_{0.7}TiO_{3+\delta}$

Fast Fourier Transform of micrograph possesses mainly the overlapped diffraction patterns of a few grains with zone axis [-111]

Bocher, L., Aguire, M. H., Robert, R., and Weidenkaff, A., *TCA* **457** (2007) 11-19.

$Sr_xEu_{1-x}TiO_{3-\delta}$

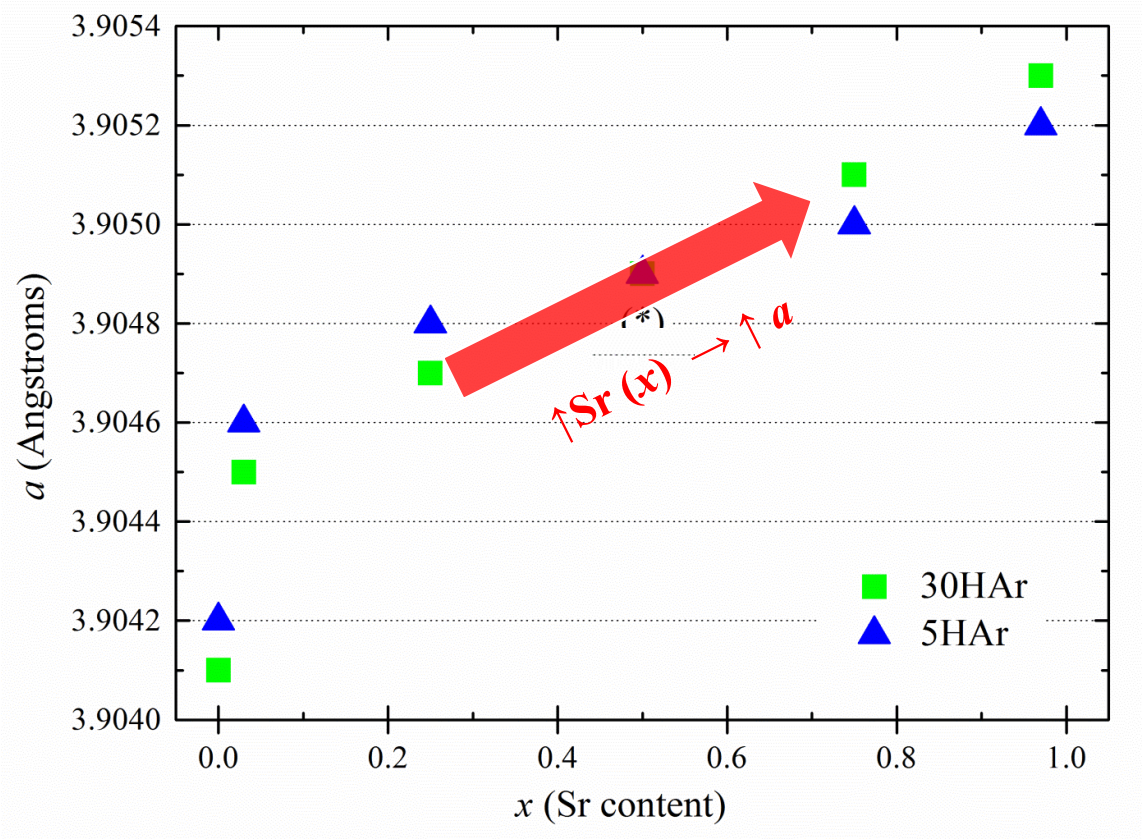

$r(Ti^{3+}) > r(Ti^{4+})$

Phase pure XRD patterns: no traces of the pyrochlore $Eu_2Ti_2O_7$ phase

↑Sr (*x*) → ↑ *a*

Sr^{2+} lower electronegativity than slightly larger ionic radius than **Eu^{2+}**

BaTi(O,N,F)

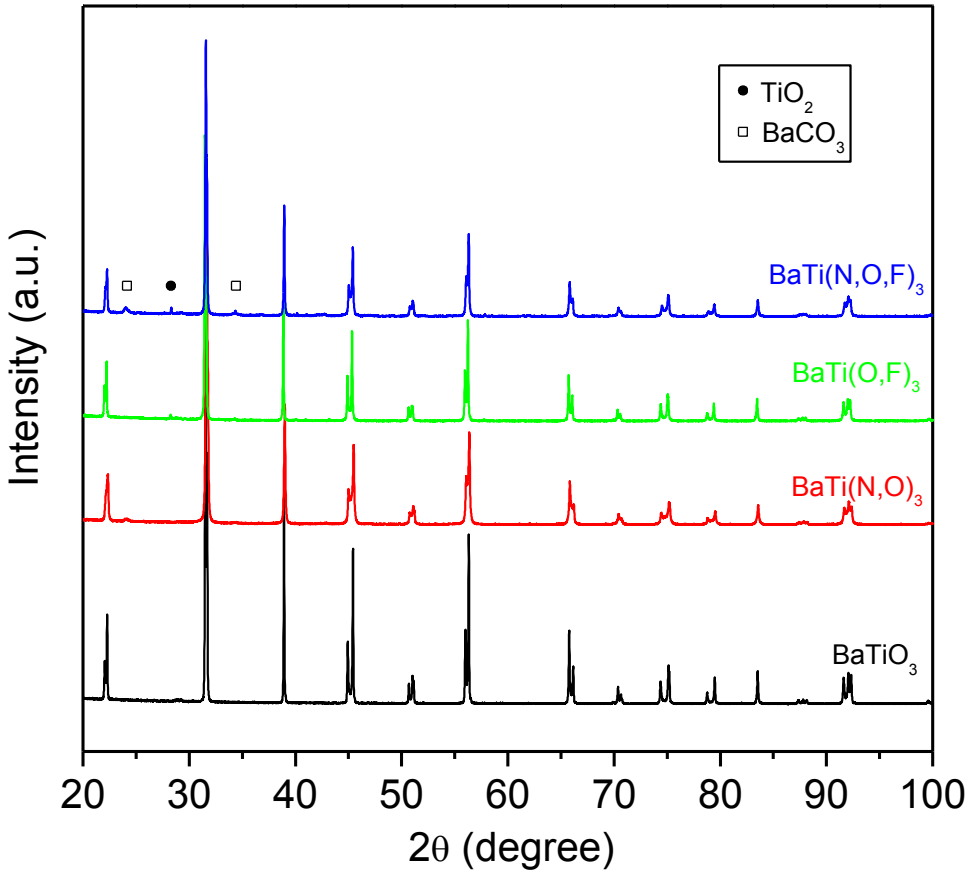
TiO2
BaCO3
BaTi(N,O,F)3
BaTi(O,F)3
BaTi(N,O)3
BaTiO3
Intensity (a.u.)
20
30
40
50
60
70
80
90
100
2θ (degree)

Mott equation for the Seebeck coefficient

$$\alpha = \frac{\pi^2 k_B^2 T}{3e}\left\{\frac{d\left[\ln(\sigma(E))\right]}{dE}\right\}_{E=E_F} = \frac{\pi^2}{3}\frac{k_B}{e}(k_B T)\left[\frac{1}{n(E)}\frac{dn(E)}{dE} + \frac{1}{\mu(E)}\frac{d\mu(E)}{dE}\right]$$

the Seebeck coefficient has two basic contributions: ***the density of states (DOS) term*** and ***the scattering mechanism term*** that intimately affects the mobility.

Brillouin zone

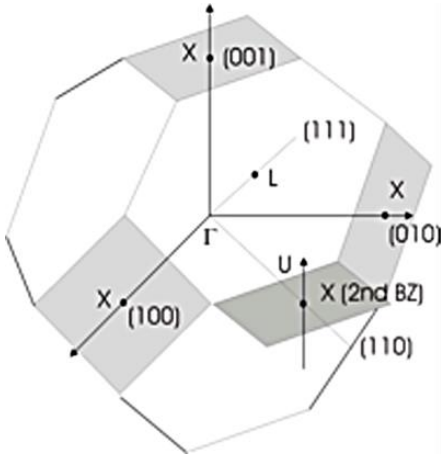

allowed states in k-space

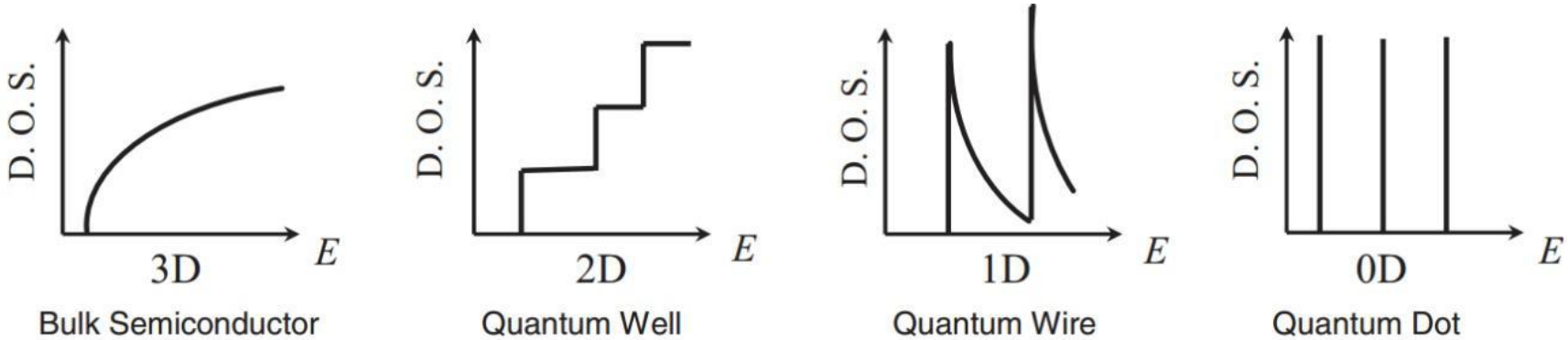

Seebeck coefficient of *Ln*$Co_{0.95}Ni_{0.05}O_3$

Heikes:

$$S(T \to \infty) = +\frac{k_B}{|e|} ln\left(\frac{1-x}{x}\right)$$

Spin-orbital entropy term

- + Spin & orbital degeneracy:

$$S(T \to \infty) = +\frac{k_B}{|e|} ln\left(\frac{g_4}{g_3}\frac{1-c_h}{c_h}\right)$$

W. Koshibae, et *al.*, PRB 62, 6869, 2000.

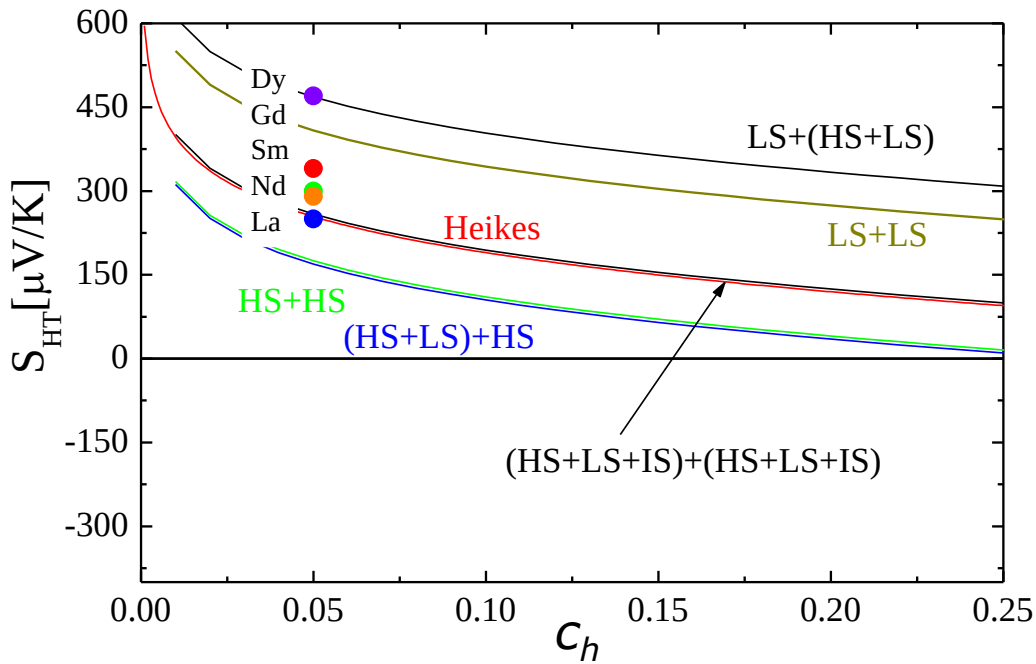

Design rules

$$ZT = \frac{S^2 \sigma}{\kappa} T$$

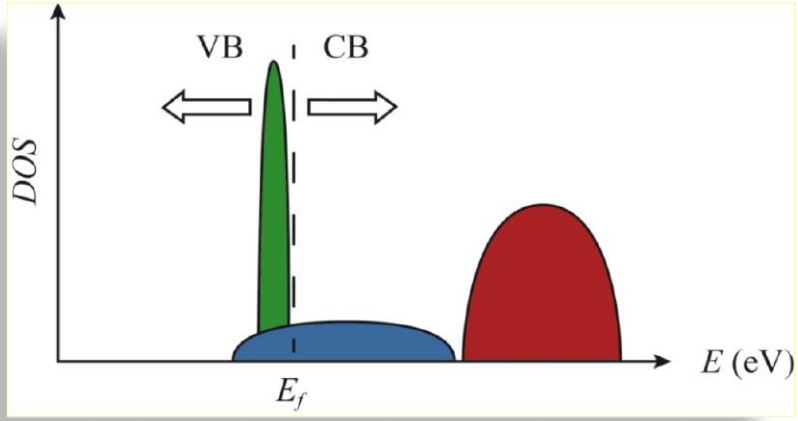

S: Large dn/dE at E = E_F
Large gap =>Low Dimensional Systems, Large Effective Mass (m*), Limit Minority Carriers, Spin entropy

σ : High charge carrier concentration and mobility
Narrow Gap, Low Electron Scattering, Correlated electrons

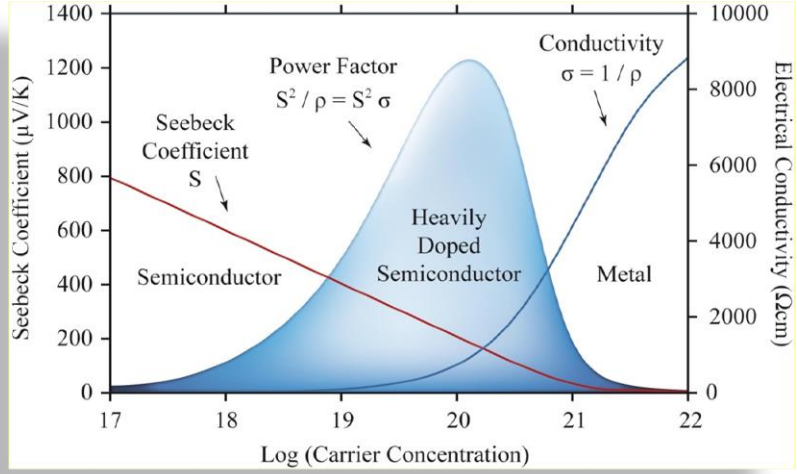

κ: Scatter Phonons, mass fluctuation, heavy atoms, Complex Structure, Defect & Grain Boundary

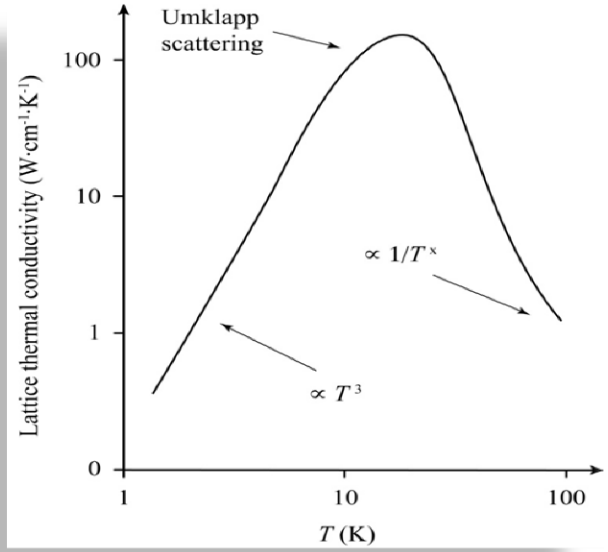

Thermocouple

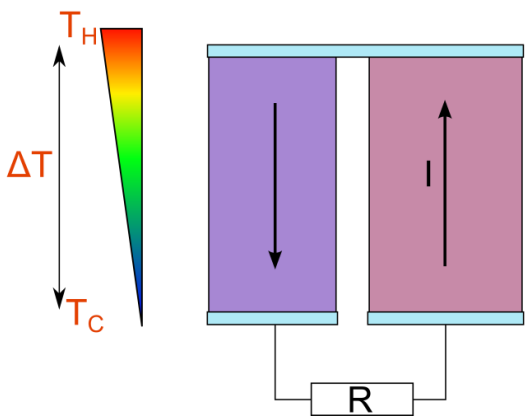

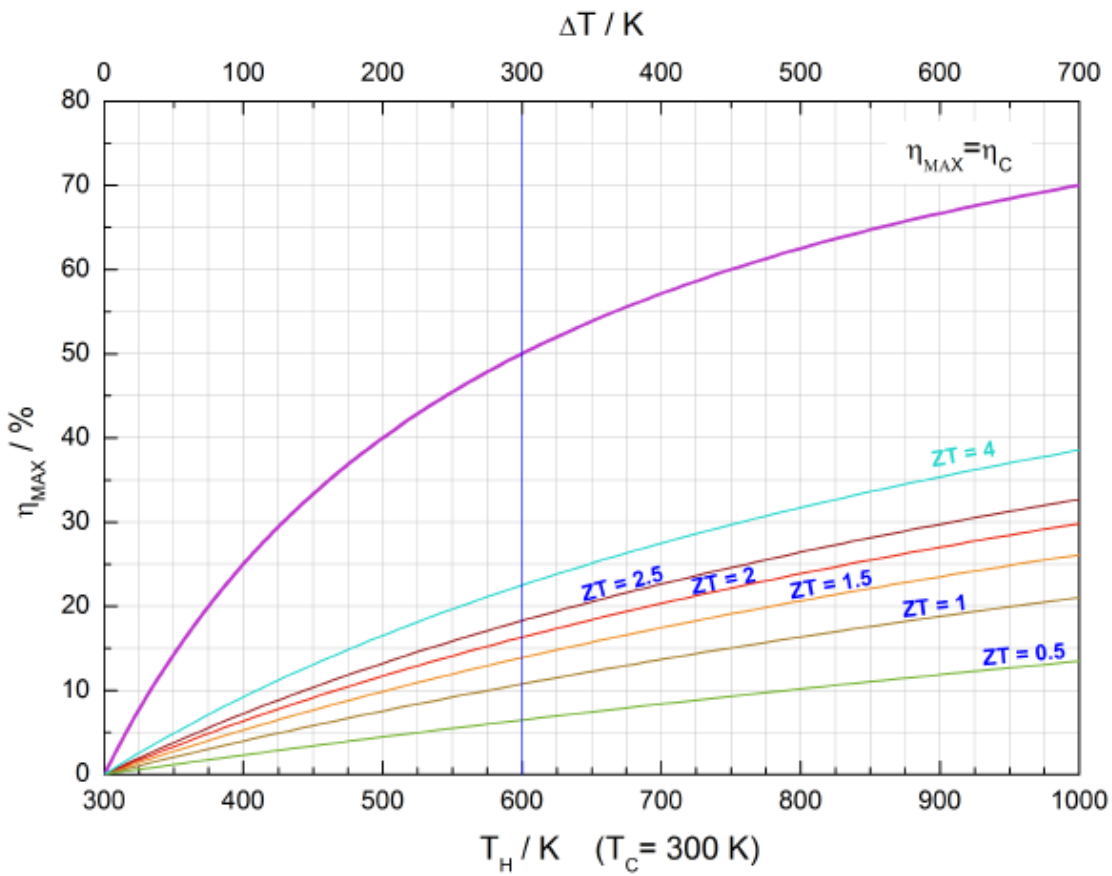

$$\eta_{max} = \eta_C \frac{\sqrt{1 + Z_{rel}\bar{T}} - 1}{\sqrt{1 + Z_{rel}\bar{T}} + \frac{T_C}{T_H}}$$

Conversion efficiency depends on the parameter $Z_{rel} = \frac{\alpha_{21}^2}{r_{12}k_{12}} = \frac{(\alpha_2 - \alpha_1)^2}{(r_1 + r_2)(k_1 + k_2)}$

Electrical resistivity and Seebeck coefficient

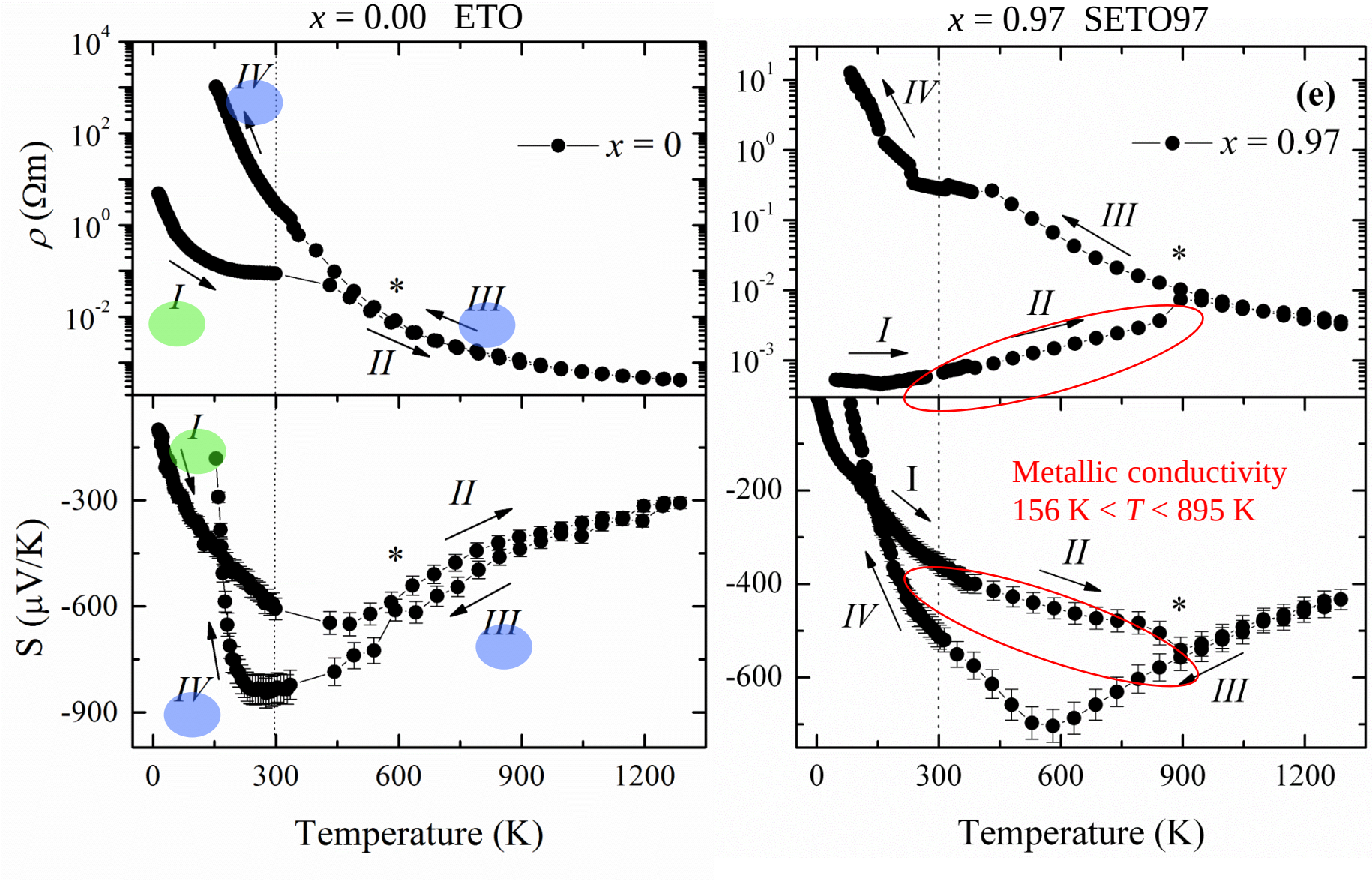

L. Sagarna et al, *J.Phys. Chem.*

Uniaxial alignment and single crystal growth

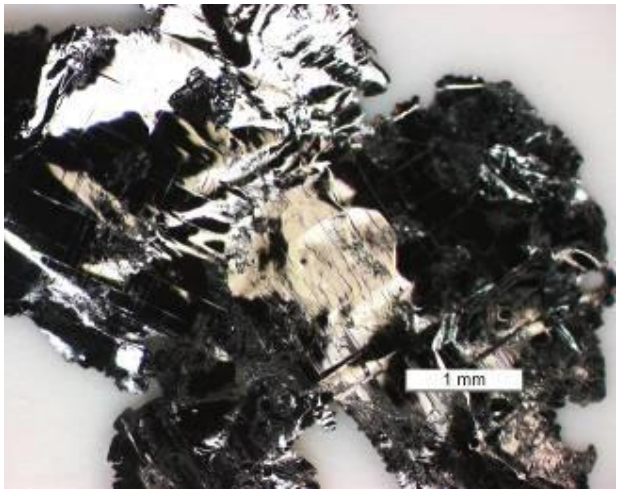

Aim:

High density
with
uniaxial alignment

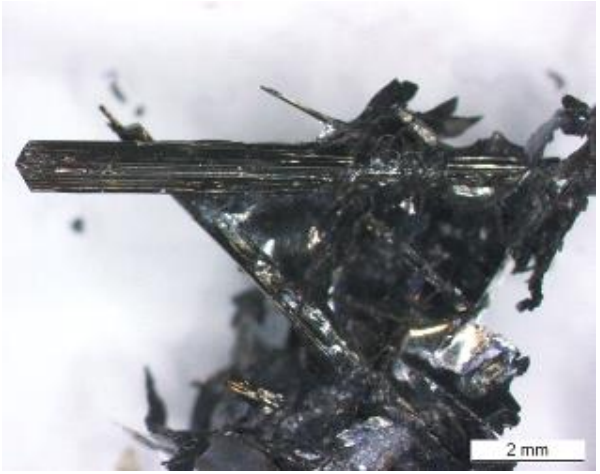

- recrystallization of Ca349 from potassium chloride/carbonate flux.

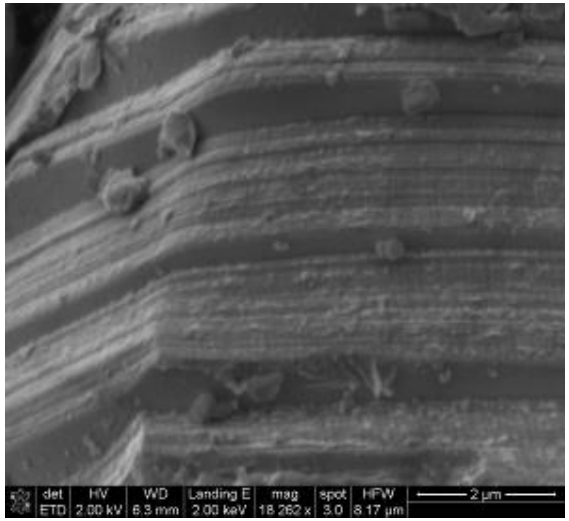

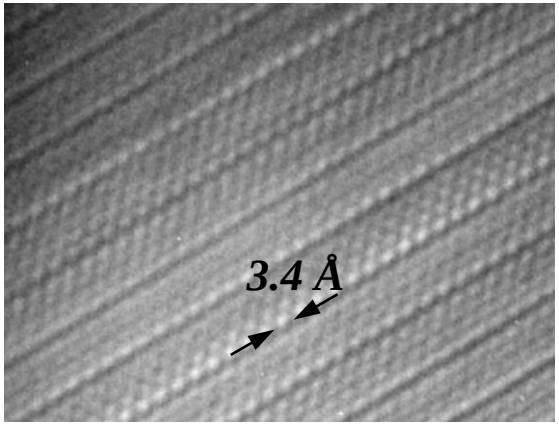

$Ca_3Co_{3.8}Fe_{0.2}O_9$

$a = 4.8Å$,
$b_1 = 4.5\ Å$,
$c = 10.8\ Å$,
$b_2 = 2.8\ Å$
$\beta \approx 98°$
$\gamma \approx 91°$

ZT of p-type «$Ca_{3-x}Bi_xCo_4O_{9+\delta}$ (0<x<0.2)»

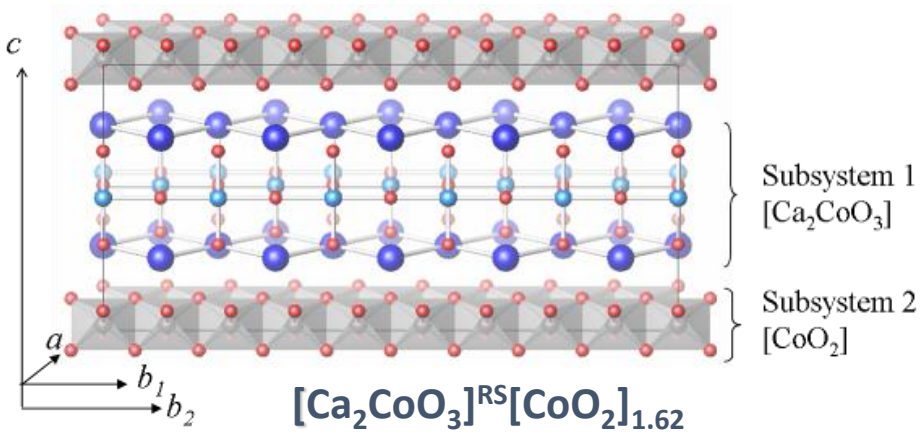

$[Ca_2CoO_3]^{RS}[CoO_2]_{1.62}$

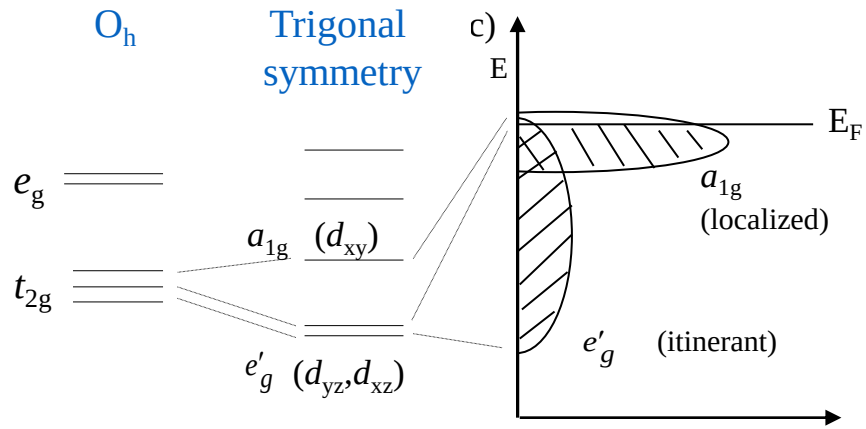

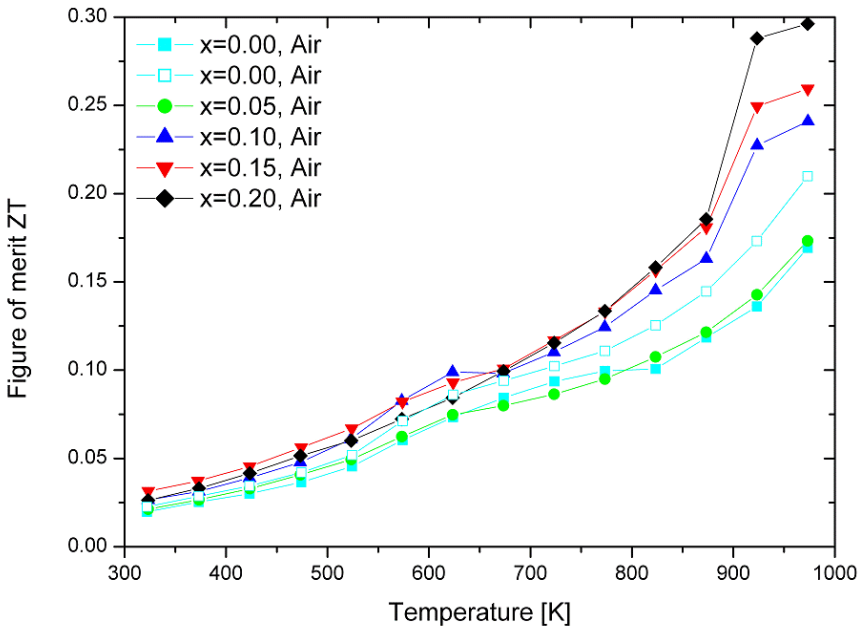

$0.3 < \delta < 0.5$

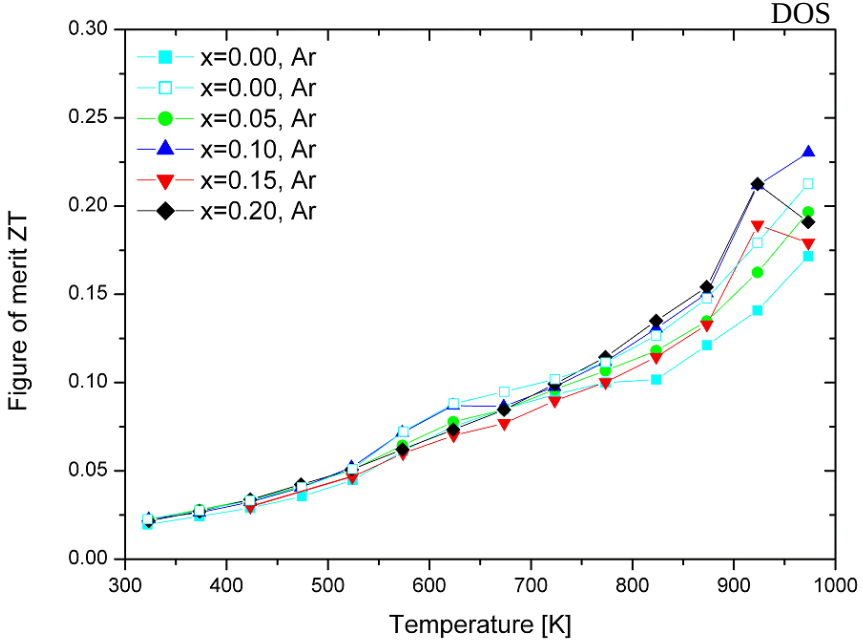

$0.0 < \delta < 0.3$

D. Moser, L. Karvonen et al, J. Solid State Sciences 13 (2011) 2160-2164

High temperature Solar Thermoelectric converters

Solar Power Concentrator

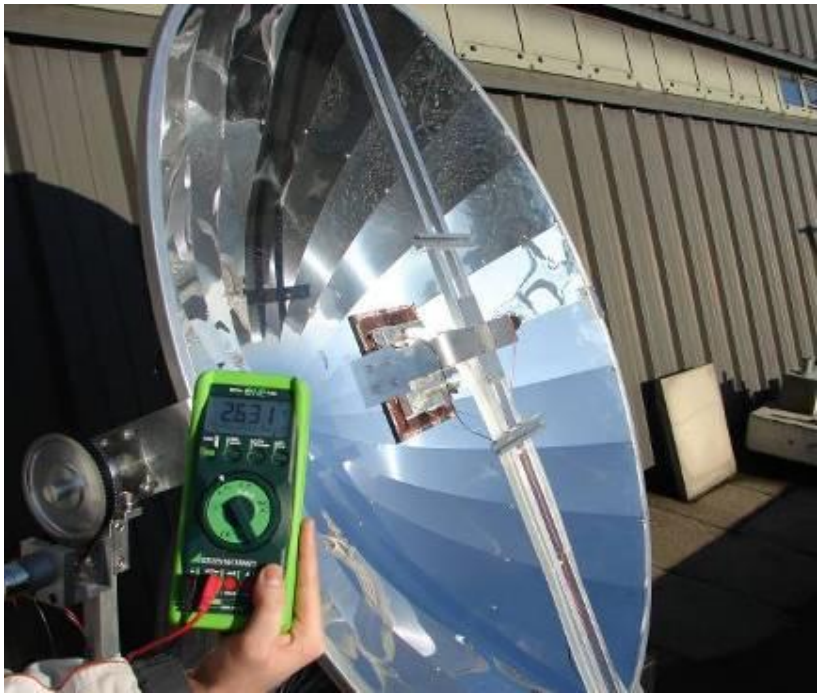

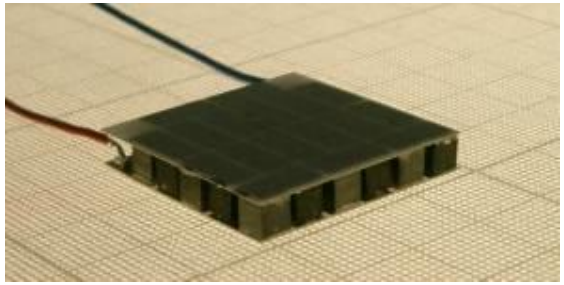

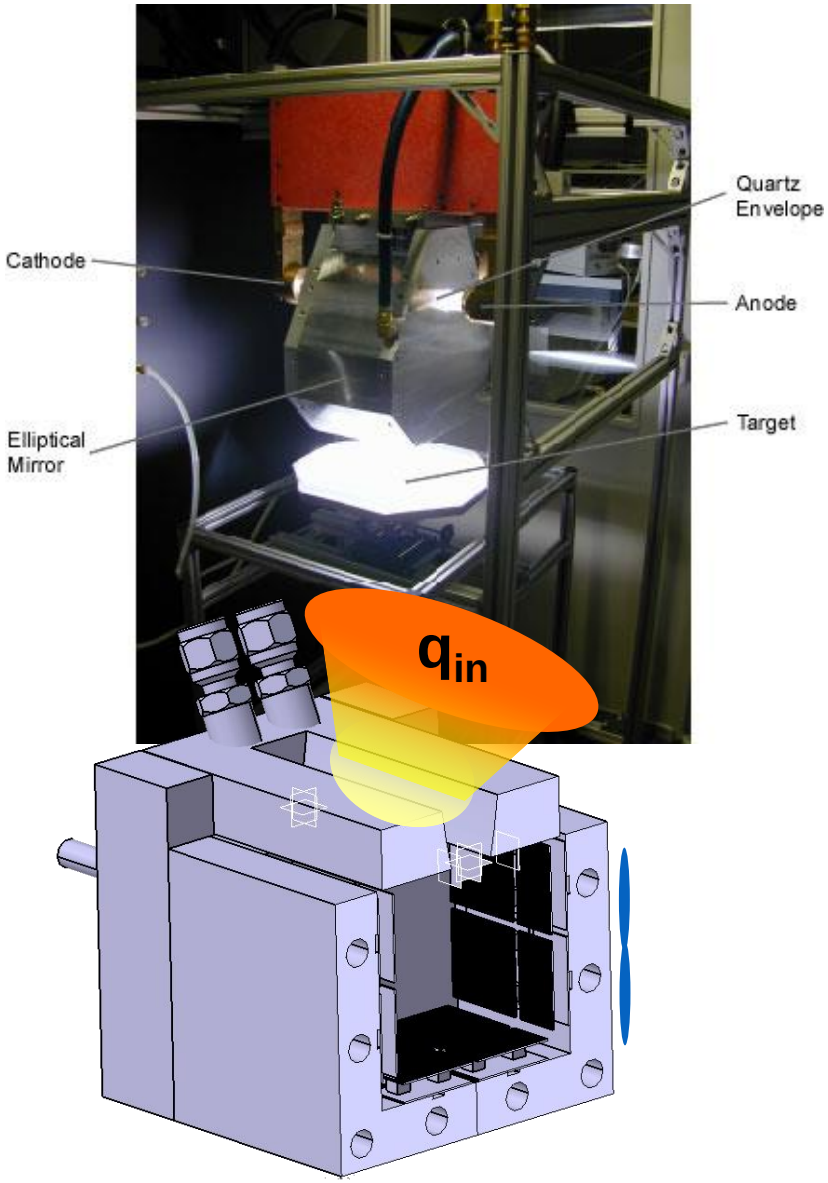

P. Tomes, C. Suter, A. Steinfeld, et al, *Materials*, **3** (2010) 2801-2814